The Astrophysical Journal, 806:200 (20pp), 2015 June 20 doi:10.1088/0004-637X/806/2/200

VARIABLE STARS AND STELLAR POPULATIONS IN ANDROMEDA XXI. II. ANOTHER MERGED GALAXY SATELLITE OF M31?*

Felice Cusano[1], Alessia Garofalo[1,2], Gisella Clementini[1], Michele Cignoni[3], Luciana Federici[1], Marcella Marconi[4], Ilaria Musella[4], Vincenzo Ripepi[4], Roberto Speziali[5], Eleonora Sani[6,7], and Roberto Merighi[1]
[1] INAF-Osservatorio Astronomico di Bologna, Via Ranzani 1, I-40127 Bologna, Italy; felice.cusano@oabo.inaf.it
[2] The Observatories of the Carnegie Institution of Washington, 813 Santa Barbara Street, Pasadena, CA 91101, USA
[3] Space Telescope Science Institute, 3700 San Martin Drive, Baltimore, MD 21218, USA
[4] INAF-Osservatorio Astronomico di Capodimonte, Salita Moiariello 16, I-80131 Napoli, Italy
[5] INAF-Osservatorio Astronomico di Roma, Via di Frascati 33, I-00040 Monte Porzio Catone, Italy
[6] INAF-Osservatorio Astronomico di Arcetri, Largo Enrico Fermi 5, I-50125 Firenze, Italy
[7] ESO, Alonso de Cordova 3107, Casilla 19001, Vitacura, Santiago 19, Chile
Received 2015 April 21; accepted 2015 May 12; published 2015 June 18

ABSTRACT

B and *V* time-series photometry of the M31 dwarf spheroidal satellite Andromeda XXI (And XXI) was obtained with the Large Binocular Cameras at the Large Binocular Telescope. We have identified 50 variables in And XXI, of which 41 are RR Lyrae stars (37 fundamental-mode—RRab, and 4 first-overtone-RRc, pulsators) and 9 are Anomalous Cepheids (ACs). The average period of the RRab stars ($\langle P_{ab} \rangle = 0.64$ days) and the period-amplitude diagram place And XXI in the class of Oosterhoff II—Oosterhoff-Intermediate objects. From the average luminosity of the RR Lyrae stars we derived the galaxy distance modulus of $(m - M)_0 = 24.40 \pm 0.17$ mag, which is smaller than previous literature estimates, although still consistent with them within 1σ. The galaxy color–magnitude diagram shows evidence for the presence of three different stellar generations in And XXI: (1) an old (∼12 Gyr) and metal-poor ([Fe/H] = −1.7 dex) component traced by the RR Lyrae stars; (2) a slightly younger (10–6 Gyr) and more metal-rich ([Fe/H] = −1.5 dex) component populating the red horizontal branch, and (3) an intermediate age (∼1 Gyr) component with the same metallicity that produced the ACs. Finally, we provide hints that And XXI could be the result of a minor merging event between two dwarf galaxies.

Key words: galaxies: dwarf – galaxies: individual (And XXI) – Local Group – stars: distances – stars: variables: general – techniques: photometric

1. INTRODUCTION

This is the second in our series of papers devoted to the study of Andromeda's (M31) satellites based on time-series photometry obtained with the Large Binocular Camera (LBC) of the Large Binocular Telescope (LBT). Our aim is to characterize the resolved stellar populations of the M31 companions using the color–magnitude diagram (CMD) and the properties of variable stars (see Clementini et al. 2011 for a general description of the project). The final goal is to derive hints on the formation history of Andromeda's satellites and relate them to the global context of merging and accretion episodes occurring in M31. Details of the survey and results from the study of the M31 satellite Andromeda XIX (And XIX) were presented in Cusano et al. (2013, hereafter Paper I). In this paper we report on the study of another very extended M31 dwarf spheroidal (dSph) companion: Andromeda XXI (And XXI). The satellite galaxies of M31 are indeed an important test-bed for both the ΛCold Dark Matter (ΛCDM) and the Modified Newtonian Dynamics (MOND; Milgrom 1983) theories. In the ΛCDM scenario the majority of the satellites are believed to be primordial dwarf galaxies residing in dark matter halos, which merge and are accreted to form larger galaxies (Zolotov et al. 2009). The satellites that we see today around M31 could thus be the residual building blocks of the M31 assembling process. However, some issues challenge the ΛCDM scenario, among them is the phase-space distribution of the satellites around M31. Ibata et al. (2013) discovered that 15 of the more than 30 satellites of Andromeda lie in a thin plane 12 kpc thick and over 200 kpc in size, which rotates around M31. Accretion of small satellites through filaments has been invoked to explain the disky distribution of these M31 companions. However, the tiny width of the disk and the large number of satellites in it are features very hard to reproduce by ΛCDM simulations (see Pawlowski et al. 2014 for a complete discussion). A different explanation for the origin of the vast thin plane of satellites orbiting M31 is that they are tidal dwarf galaxies formed in the debris of a past major merger between M31 and a massive galaxy (Hammer et al. 2013). The space distribution of the satellites is well reproduced by numerical models of galaxy interaction. A further alternative to the merger model is that the satellites formed during a past flyby of the Milky Way (MW) and M31 about 10 Gyr ago. Indeed, under the assumption of Milgromiam dynamics,[8] Zhao et al. (2013) found that M31 and the MW had a close flyby encounter between 7 and 11 Gyr ago. Understanding the real nature/origin of the M31 satellites is thus crucial to address cosmological theories.

And XXI was discovered by Martin et al. (2009) in the context of the PAndAS survey (Martin et al. 2013 and references therein). The discovery paper reports a distance modulus of $(m - M)_0 = 24.67 \pm 0.13$ mag from the luminosity of the red giant branch (RGB) tip and a half-light radius (r_h) of 3′.5 (corresponding to $r_h = 875 \pm 127$ pc at the distance of And XXI). This makes And XXI the fourth largest dSph in the Local Group (LG). The galaxy has a metallicity of

* Based on data collected with the LBC at the LBT.

[8] Milgrom (1983).

Table 1
Log of And XXI Observations

Dates	Filter	N	Exposure Time (s)	Seeing (FWHM) (arcsec)
2010 Oct 8–11,	*B*	6	420	1.4
2010 Dec 1–3,	*B*	40	420	0.8
2010 Oct 8–11,	*V*	7	420	1.4
2010 Dec 1–3,	*V*	39	420	0.8

[Fe/H] $= -1.8 \pm 0.4$ dex, as estimated by Collins et al. (2013) from the calcium triplet (CaII) of the galaxy red giants. The same authors measured a velocity dispersion of $\sigma = 4.5^{+1.2}_{-1.0}$ kms^{-1} from 32 spectroscopically confirmed members, which is rather low, when compared with the great extension of And XXI. This was interpreted by Collins et al. (2013) as the result of a possible past tidal interaction with M31; however, for McGaugh & Milgrom (2013) the low dispersion naturally arises in the MOND context. Conn et al. (2012) adopting a bayesian approach to locate the galaxy RGB tip have revised

Table 2
Identification and Properties of the Variable Stars Detected in And XXI

Name	α (2000)	δ (2000)	Type	P (days)	Epoch (max) JD (−2455000)	$\langle B \rangle$ (mag)	$\langle V \rangle$ (mag)	A_B (mag)	A_V (mag)
V1	23:54:47.066	+42:28:19.42	RRc	0.3950	533.684	25.87	25.38	0.66	0.51
V2	23:54:47.688	+42:27:16.38	RRab	0.6085	533.658	25.96	25.57	1.00	1.29
V3	23:54:49.205	+42:29:15.29	RRab	0.5810	477.692	25.77	25.30	1.21	0.95
V4	23:54:46.450	+42:27:09.43	AC	1.2353	532.625	24.22	23.63	1.33	1.03
V5	23:54:46.788	+42:29:24.59	RRab	0.6708	533.608	25.74	25.22	0.99	0.77
V6	23:54:51.778	+42:27:37.58	AC	1.067	476.959	24.63	24.07	1.06	0.53
V7	23:54:49.066	+42:29:24.25	RRab	0.6132	532.665	25.84	25.38	1.11	0.78
V8	23:54:46.471	+42:29:37.67	RRab	0.8342	531.621	25.55	24.93	0.83	0.8
V9	23:54:42.230	+42:27:49.18	RRc	0.3869	532.718	26.02	25.52	0.60	0.37
V10	23:54:53.642	+42:27:45.65	RRab	0.6371	532.605	25.82	25.33	0.87	0.57
V11	23:54:39.698	+42:29:12.73	RRab	0.6210	533.745	25.82	25.21	0.96	0.81
V12	23:54:49.212	+42:30:26.64	RRab	0.6662	533.727	25.85	25.31	1.25	1.06
V13	23:54:40.649	+42:26:34.55	AC	1.138	533.754	24.53	24.09	1.66	1.34
V14	23:54:38.774	+42:29:26.20	AC	1.072	533.590	24.96	24.44	1.18	0.85
V15	23:54:52.061	+42:30:34.56	AC	1.715	477.670	24.15	23.63	1.27	0.99
V16	23:54:38.664	+42:26:52.66	RRab	0.643	533.510	25.78	25.31	1.30	1.15
V17	23:54:56.498	+42:30:06.08	RRab	0.5768	532.663	25.78	25.26	1.30	1.08
V18	23:54:36.979	+42:29:18.24	RRab	0.5785	533.691	25.80	25.30	1.25	1.00
V19	23:54:36.562	+42:27:21.82	AC	1.390	531.670	24.27	23.80	1.32	1.00
V20	23:54:52.507	+42:30:56.59	RRab	0.6193	532.710	25.99	25.41	0.83	0.64
V21	23:54:37.603	+42:30:16.38	RRab	0.5971	533.717	25.84	25.32	1.19	0.92
V22	23:54:54.931	+42:31:04.19	RRab	0.5911	532.740	25.87	25.36	0.78	0.63
V23	23:54:35.311	+42:29:34.87	RRab	0.6661	531.686	25.74	25.21	1.24	1.05
V24	23:54:59.700	+42:26:26.59	RRab	0.6019	531.690	25.87	25.37	1.08	0.79
V25	23:54:33.816	+42:27:37.80	RRab	0.6368	531.750	25.93	25.42	0.86	0.76
V26	23:55:01.913	+42:28:29.10	AC	1.1500	480.518	24.05	23.58	1.19	0.94
V27	23:55:01.992	+42:28:35.47	RRab	0.7052	480.660	25.60	25.04	0.59	0.46
V28	23:54:59.134	+42:26:03.77	RRc	0.3058	533.711	25.68	25.34	0.76	0.56
V29	23:55:01.531	+42:27:10.69	RRab	0.6414	532.605	25.78	25.28	0.78	0.60
V30	23:54:45.857	+42:24:38.95	RRab	0.5898	531.768	25.74	25.28	1.33	1.12
V31	23:55:02.167	+42:27:34.31	RRab	0.5880	533.640	25.74	25.31	0.85	0.80
V32	23:55:01.817	+42:29:23.64	RRab	0.6513	533.530	25.79	25.38	1.12	0.86
V33	23:54:52.793	+42:24:41.00	RRab	0.6182	533.750	25.95	25.41	1.20	0.89
V34	23:54:39.821	+42:31:39.79	AC	1.2460	532.702	24.45	24.01	1.30	0.98
V35	23:54:44.129	+42:32:06.32	RRab	0.6061	532.770	25.92	25.31	1.13	0.88
V36	23:54:47.352	+42:32:16.44	RRab	0.6167	480.650	25.88	25.37	0.94	0.77
V37	23:54:34.003	+42:30:25.91	RRab	0.7074	532.768	25.77	25.26	0.84	0.79
V38	23:54:57.665	+42:31:48.01	RRc	0.2851	532.700	25.89	25.45	0.63	0.39
V39	23:54:35.669	+42:31:30.14	RRab	0.5707	477.705	25.87	25.38	1.02	0.91
V40	23:54:47.770	+42:23:10.75	RRab	0.7178	532.760	25.77	25.28	0.82	0.64
V41	23:54:45.545	+42:33:18.90	RRab	0.5860	531.715	25.89	25.45	1.24	0.87
V42	23:54:39.228	+42:23:22.13	RRab	0.6824	531.748	25.70	25.21	1.17	0.85
V43	23:54:36.629	+42:33:24.98	RRab	0.6078	531.747	25.88	25.35	1.16	0.91
V44	23:55:04.075	+42:32:50.46	AC	1.1655	477.405	24.21	23.82	1.12	0.87
V45	23:54:43.080	+42:21:30.78	RRab	0.5670	533.650	25.80	25.34	1.17	1.03
V46	23:55:14.446	+42:31:01.42	RRab	0.71:	533.726	25.89	25.30	0.81	0.63
V47	23:55:16.555	+42:28:51.39	RRab	0.5646	532.655	25.84	25.34	1.51	1.17
V48	23:55:21.782	+42:29:46.14	RRab	0.7560	532.795	25.83	25.36	0.68	0.61
V49	23:53:54.898	+42:25:56.04	RRab	0.6766	532.652	25.79	25.29	0.94	0.73
V50	23:55:46.274	+42:26:55.86	RRab	0.6920	531.762	25.84	25.39	0.80	0.57

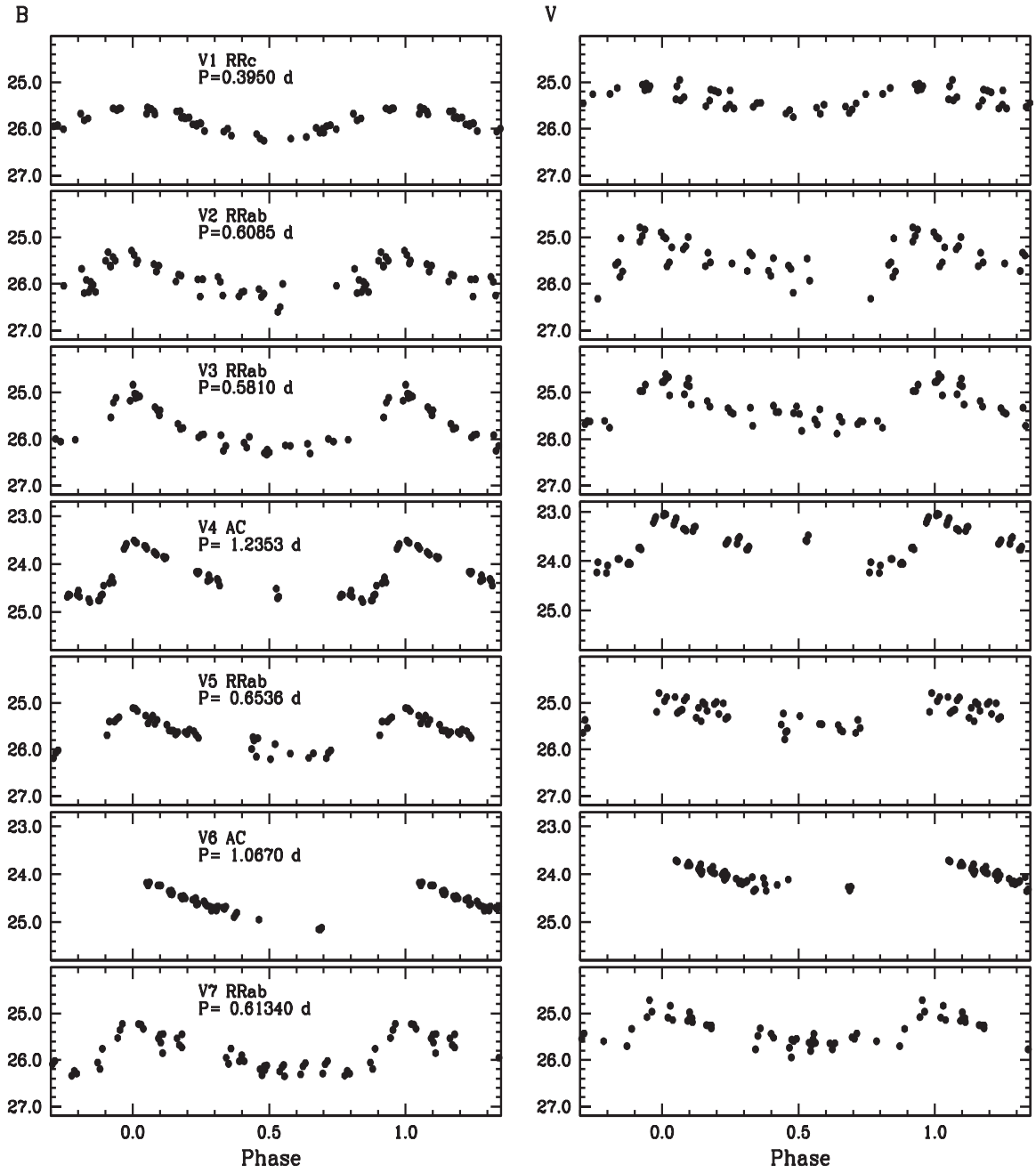

Figure 1. *B* (left panels) and *V* (right panels) light curves of the variable stars identified in And XXI. Stars are ordered by increasing the distance from the galaxy center, for which we adopted Martin et al. (2009) coordinates. Typical internal errors for the single-epoch data are in the range of 0.02–0.18 mag in *B*, and of 0.03–0.25 mag in *V*.

the And XXI distance modulus to $(m-M)_0 = 24.59^{+0.06}_{-0.07}$ mag, which, although shorter, is still within 1σ of Martin et al. (2009)'s value.

The paper is organized as follows. Observations, data reduction, and calibration of And XXI photometry are presented in Section 2. Results on the identification and characterization of the variable stars, the catalog of light curves, and the Oosterhoff classification of And XXI are discussed in Sections 3. The distance to And XXI derived from the RR Lyrae stars is presented in Section 4. The galaxy CMD is discussed in Section 5 and the *projected* distribution of And XXI stellar components is given in Section 6. Section 7 gives some hints on the possibility of a past merging. Finally, a summary of the main results is presented in Section 8.

2. OBSERVATIONS AND DATA REDUCTION

Time-series photometry in the *B* and *V* bands of a $23' \times 23'$ region centered on And XXI (R.A. $= 23^{\rm h}54^{\rm m}47\overset{\rm s}{.}7$, decl. $= +42°28'15''$, J2000.0; Martin et al. 2009) was obtained in 2010 October and December with the LBC at the foci of the LBT. Sub-arcsec seeing conditions were achieved for the December observations, while seeing was slightly worse during the October run. Observations in the *B* band were obtained with

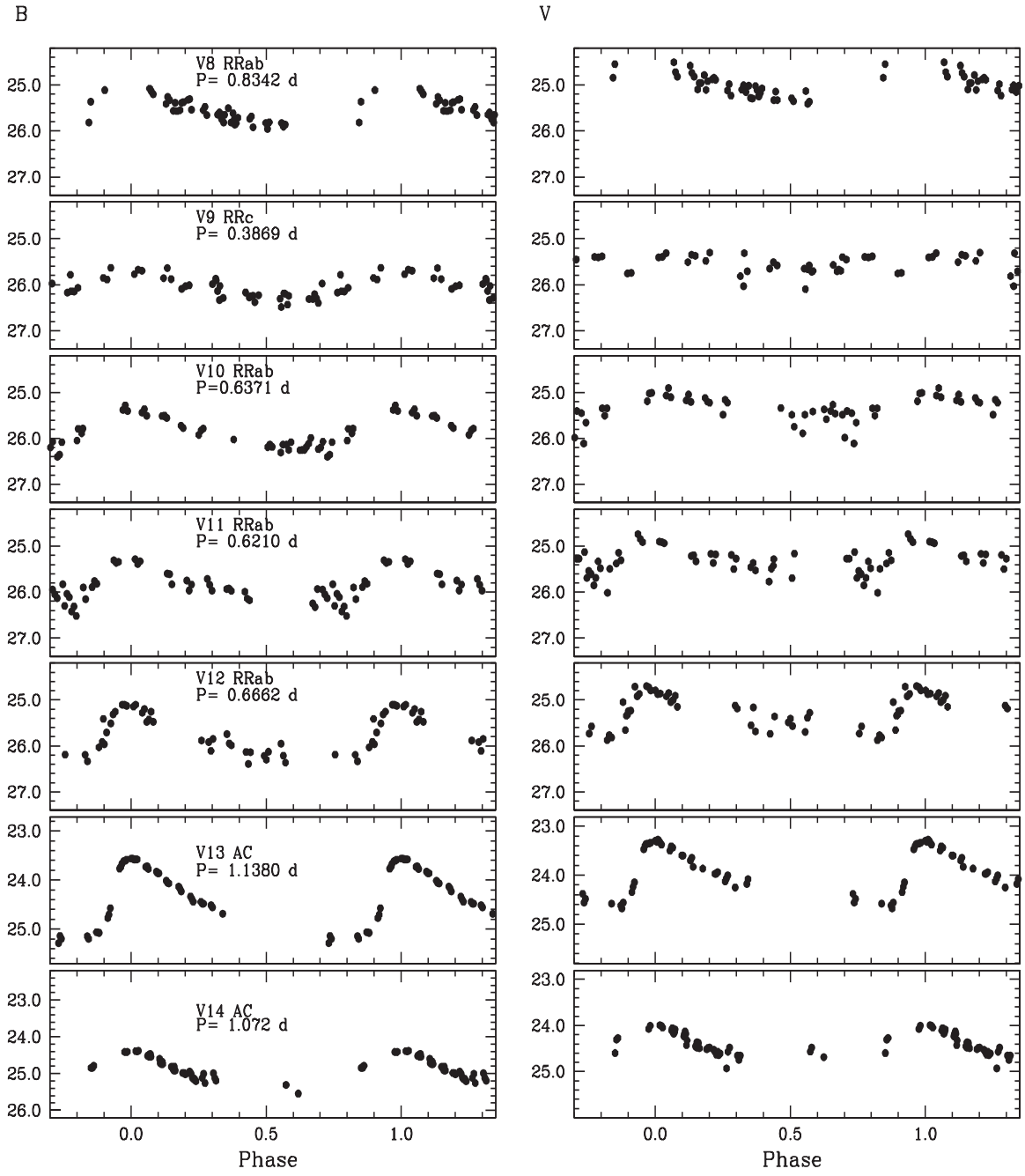

Figure 1. (Continued.)

the Blue camera of the LBC, whereas the *V* images were acquired with the Red camera. A total of 46 *B* and 46 *V* images each of 420 s exposure were obtained for a total exposure time of 19,320 s in each band. Images in both bands were dithered by 30 arcsec in order to fully cover the inter-CCD gaps of the LBC mosaic. Observations of And XIX were obtained in the same nights by interchanging the two targets in order to evenly sample the light curves of variable stars possibly occurring in the two galaxies. The log of the observations of And XXI is provided in Table 1. Data reduction was performed in the same way as for And XIX and is described in Paper I, to which the interested reader is referred for details. The PSF photometry was performed using the DAOPHOT-ALLSTAR-ALLFRAME package (Stetson 1987, 1994). Since the observations of And XXI were acquired within a few minutes from those of And XIX for the absolute photometric calibration, we used the calibrating equations derived in Paper I, by properly accounting for differences in airmass between the two targets.

3. VARIABLE STARS

Identification of the variable stars was performed using the variability index computed in DAOMASTER (Stetson 1994), then the light curves of the candidate variables were analyzed with the Graphical Analyzer of Time Series (GRATIS), custom software developed at the Bologna Observatory by P.

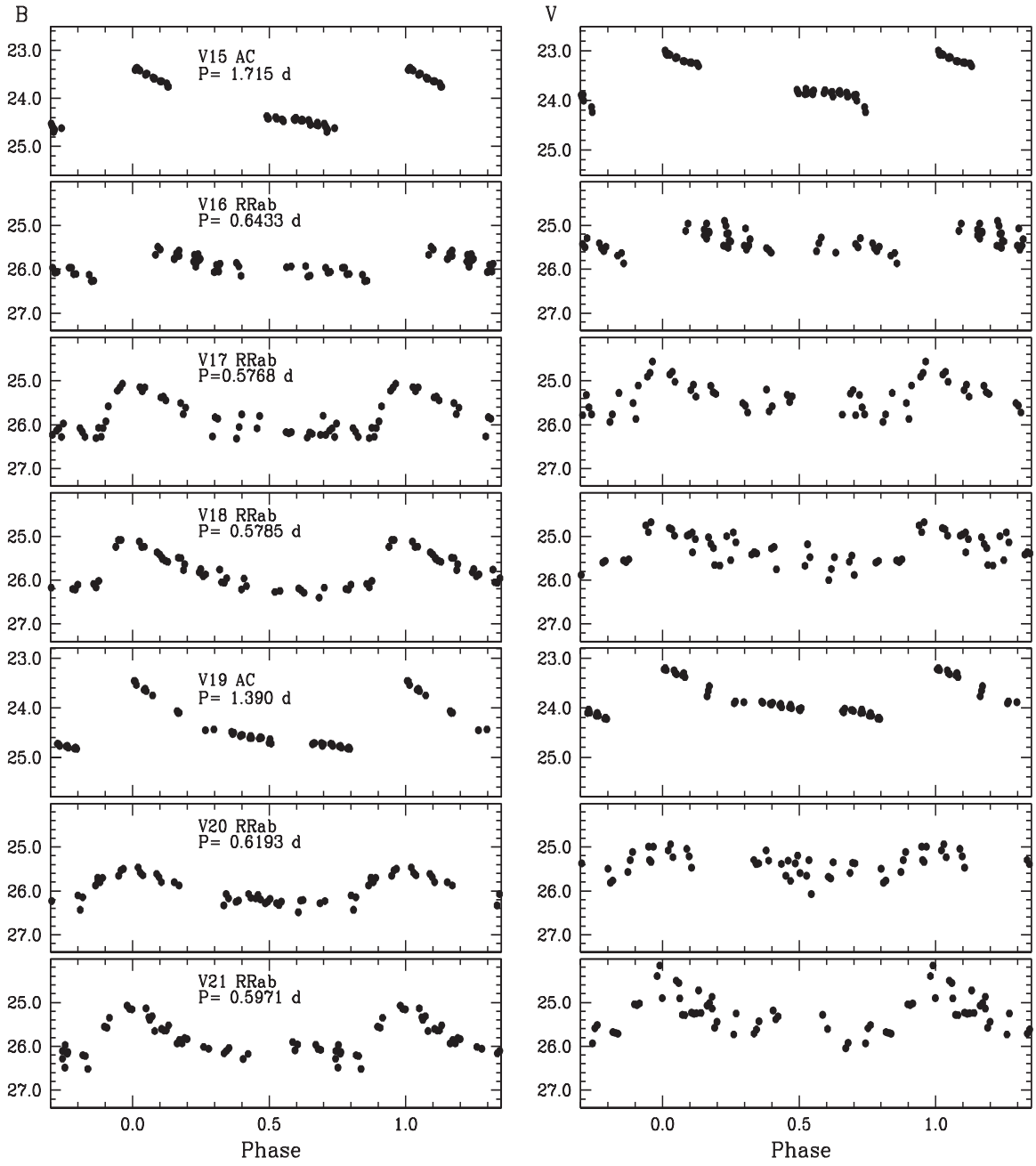

Figure 1. (Continued.)

Montegriffo (see, e.g., Clementini et al. 2000). Further details on the search for variables and the analysis of the light curves can be found in Paper I. A total of 50 variable stars were identified both in the *B* and *V* band data sets. The properties of the variable stars detected in And XXI are summarized in Table 2. We named the variables with an increasing number starting from the galaxy center, for which we adopted the coordinates by Martin et al. (2009). Column 1 gives the star identifier, Columns 2 and 3 provide the R.A. and decl. (J2000 epoch), respectively. These coordinates were obtained from our astrometrized catalogs. Column 4 gives the type of variability. Columns 5 and 6 list the period and the Heliocentric Julian Day of maximum light, respectively. Columns 7 and 8 give the intensity-weighted mean *B* and *V* magnitudes, while Columns 9 and 10 list the corresponding amplitudes of the light variation. Light curves are presented in Figure 1.

3.1. RR Lyrae Stars

We discovered a total of 41 RR Lyrae stars in And XXI, of which 37 are RRab and 4 RRc pulsators. The average period of the 37 bona fide RRab stars is $\langle P_{ab} \rangle = 0.64$ days ($\sigma = 0.06$ days). Considering only RRab stars inside the galaxy half-light radius the average period becomes $\langle P_{ab} \rangle = 0.63$ days ($\sigma = 0.05$ days, average on 22 stars). From the average period of the RRab stars, And XXI can be classified as an Oosterhoff II (Oo II)/ Osterhoff Intermediate

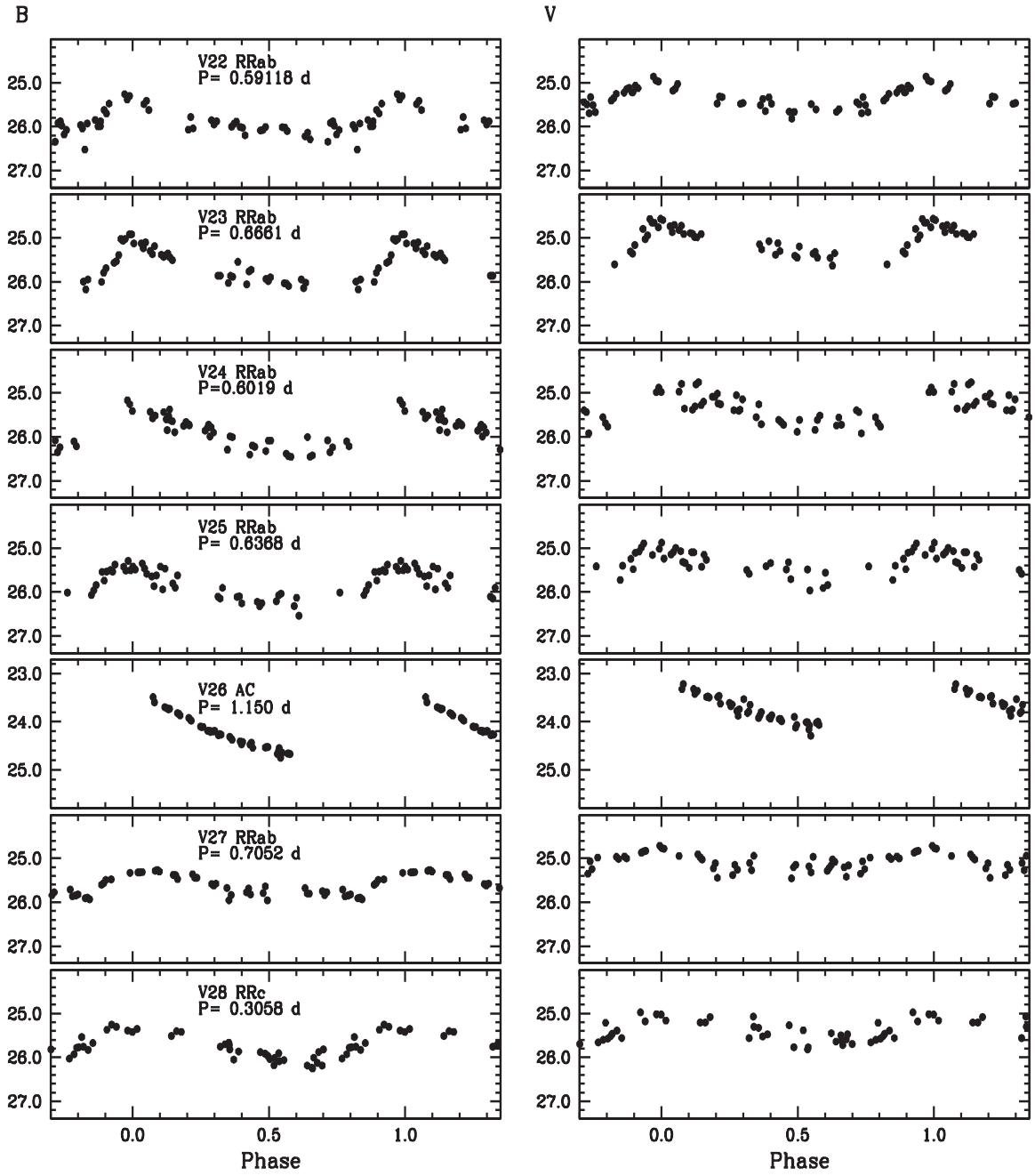

Figure 1. (Continued.)

(Oo Int) object (Oosterhoff 1939). However, since the rms of the average period is rather large, in order to better investigate the Oosterhoff nature of And XXI we produced the histogram of the RR Lyrae periods. This is shown in Figure 2. A multi-Gaussian fit was performed to find the peak value of this distribution. We found two separate maxima, a first higher peak is at $P_1 = 0.60$ days with $\sigma = 0.02$ days and contains about 36% of the RR Lyrae stars, and a second one at $P_2 = 0.68$ days with $\sigma = 0.03$ days and about 24% of the variables. The fit is shown in Figure 2. The presence and relative strength of these two peaks reinforces for And XXI a classification as Oo Int/Oo II object. In the histogram two RR Lyrae stars, V8 and V48, show longer periods when compared to the average distribution. We comment on these stars further in Section 3.3.

The period-amplitude diagram (also known as the Bailey diagram; Bailey 1902) of the And XXI RR Lyrae stars is shown in Figure 3 together with the loci defined by bona fide regular (solid line) and the well-evolved (dashed line) RR Lyrae stars in the Galactic globular cluster M3, according to Cacciari et al. (2005). M3 regular RR Lyrae stars have Oosterhoff I (Oo I) properties, while the M3 evolved variables mimic the location of the Oo II variables. The majority of the And XXI RR Lyrae stars fall between the two loci and near the position of the Oo II locus, thus confirming the galaxy classification as an Oo Int/Oo II object. The fraction of RRc stars over the total number of RR Lyrae stars is $f_c = N_c/N_{\rm ab+c} = 0.10$, that is small both for an Oo II ($f_c \sim 0.44$) and an Oo I ($f_c \sim 0.17$) system. This fraction is also small compared to

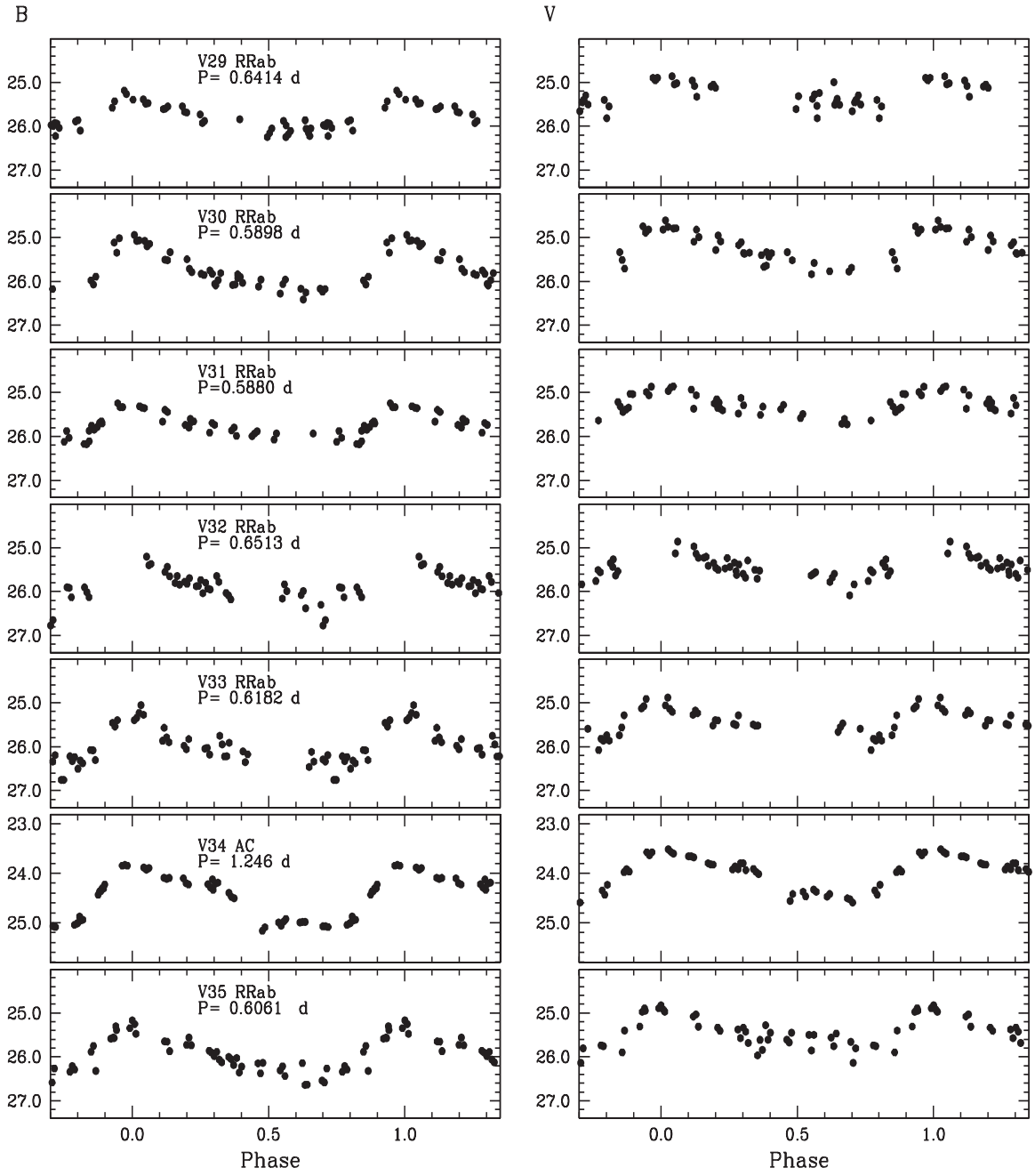

Figure 1. (Continued.)

other dwarf galaxies of similar metallicity (Fe/H $= -1.8$ dex; Collins et al. 2013) like for example And XIX ($f_c = 0.26$; Paper I). RRc stars have smaller amplitudes, hence they are more difficult to identify than RRab stars. Furthermore, they have bluer colors. Hence, as it will be discussed in Section 5, they occur in the region of the CMD that is heavily contaminated by background galaxies. This could affect our capability of detecting RRc stars. However, we individually checked for variability all stars bluer than $B - V \sim 0.40$ mag in the horizontal branch (HB) region of the CMD and did not find additional variables. Furthermore, in And XIX as well as in other M31 dSphs we are studying, we do find RRc stars, in spite of the contamination by background galaxies in that part of the CMD. Hence, we are inclined to think that the paucity of first overtone (FO) pulsators in And XXI is a real feature.

The spatial distribution of the RR Lyrae stars is shown in Figure 4 (filled red circles), and indicates a rather complex structure for And XXI. The RR Lyrae stars seem to be asymmetrically distributed. In particular, outside the galaxy half-light radius we note two elongated features traced by the variable stars, one ~12 arcmin long going from north–west to south–east and the other pointing toward south. They may trace past interactions with a dwarf satellite galaxy of M31 and/or with M31 itself. We discuss this in more detail in Section 5.

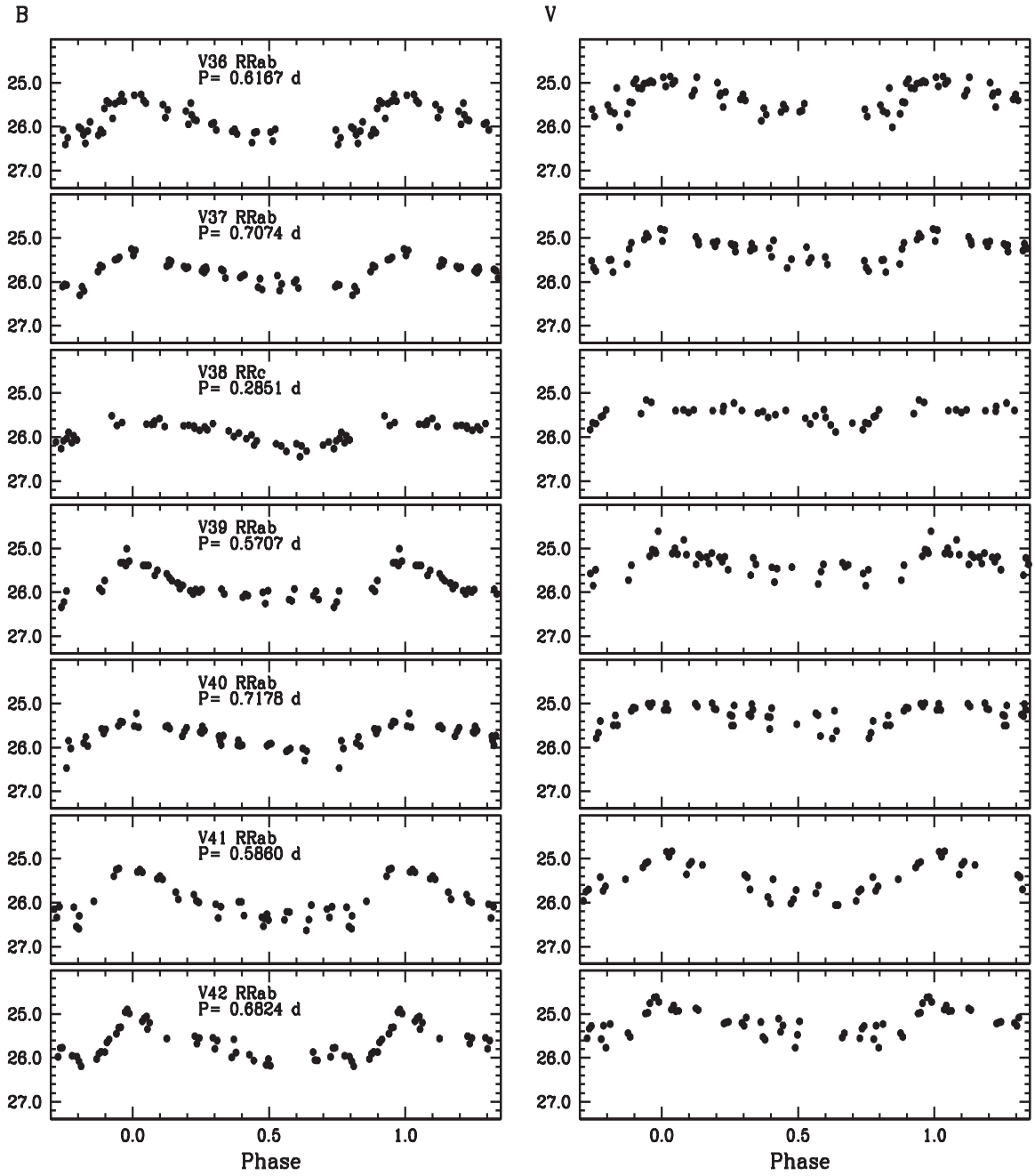

Figure 1. (Continued.)

3.2. Anomalous Cepheids

We found in And XXI nine variable stars that are ∼1 mag brighter than the average magnitude of the RR Lyrae stars. We classified these stars as Anomalous Cepheids (ACs) based on the comparison with stellar isochrones and the period-Wesenheit (PW) relation of ACs. The Wesenheit function (van den Bergh 1975; Madore 1982) is defined as $W(B, V) = M_V - 3.1 \times (B - V)$, where M_V is the V magnitude corrected for the distance. The $\langle V \rangle$ magnitudes of the ACs were corrected adopting the distance modulus $(m - M)_0 = 24.40 \pm 0.17$ mag derived from the RR Lyrae stars (see Section 4) and used to derive the corresponding Wesenheit indices. The PW relations of And XXI ACs are shown in the left panel of Figure 5 along with the PW relation for Fundamental (F) mode and FO mode ACs recently derived for the LMC (solid lines) by Ripepi et al. (2014).[9] The nine ACs in And XXI well follow, within the errors, the Ripepi et al. (2014) relations for F and FO pulsators. To confirm that these bright variables are mostly ACs, in the right panel of Figure 5 we compare them with the PW relation for Classical Cepheids (CCs) in the LMC derived by Soszynski et al. (2008). The PW relations for CCs indeed do not fit very well the bright variables in And XXI. However,

[9] Ripepi et al. (2014)'s relations were derived for the V and I bands, and we have converted them to B and V using Equation (12) of Marconi et al. (2004).

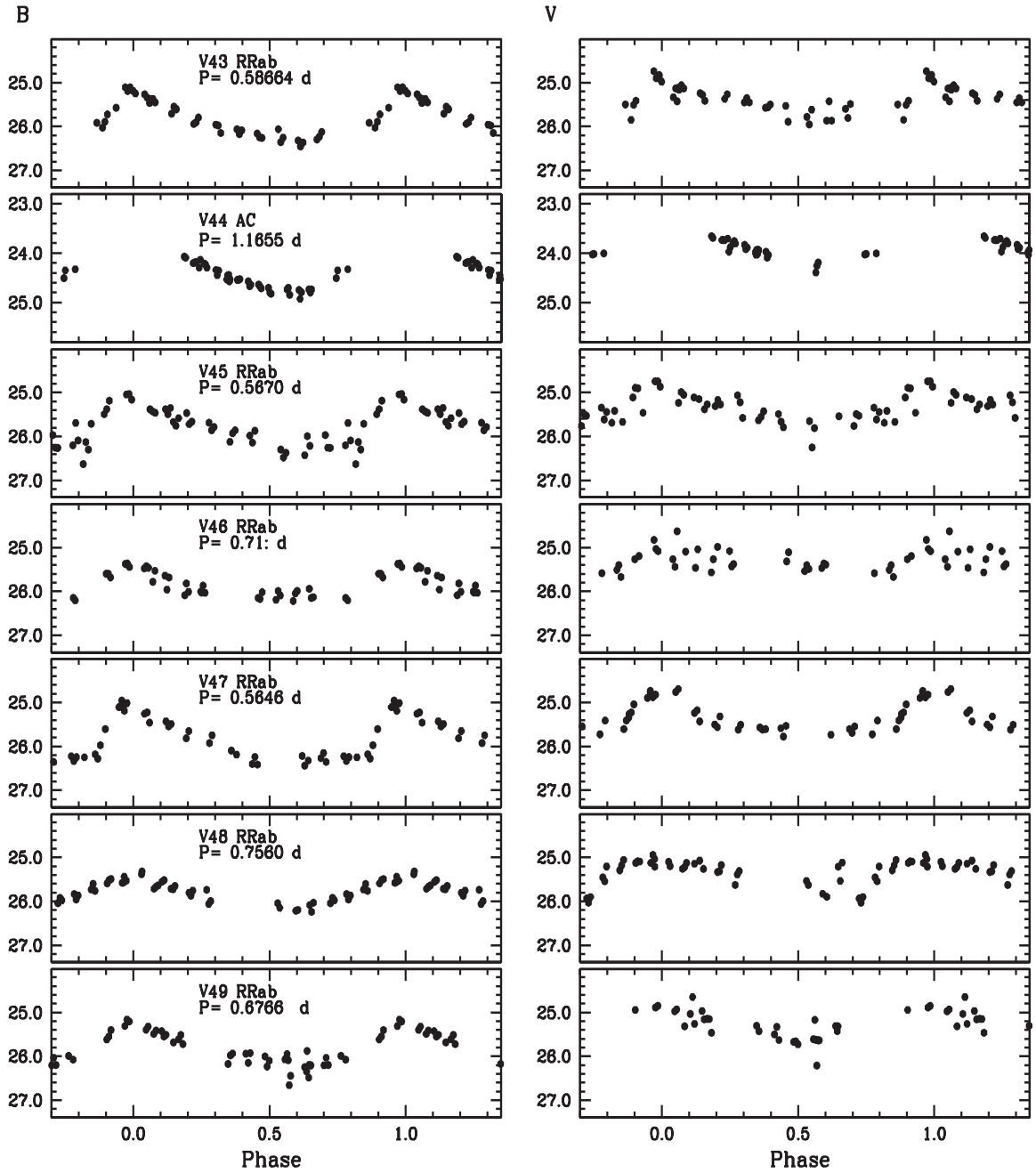

Figure 1. (Continued.)

we cannot totally reject the possibility that at least one, perhaps two, of the bright variables (namely, V4 and V26) could be CCs. As in Paper I we derived the specific frequency of ACs in the galaxy, on the assumption that all the nine bright variables in And XXI are bona fide ACs. This is plotted in Figure 6 along with the AC specific frequency in a number of MW and M31 dwarf satellites. And XXI (starred symbol in Figure 6) well follows the relation traced by the other dwarf galaxies. The error is computed considering Poisson statistics and includes the case in which two of the ACs are in fact CCs.

3.3. Comments on Individual Peculiar Stars

V2—The star is 0.3 mag fainter than the average V magnitude of RR Lyrae stars. The pulsation amplitude in the V band is larger than in the B band, and the V light curve although well sampled is very noisy. The color of the star is blue ($(B - V) = 0.39$ mag) for an RRab. Only V28 which is an RRc star, is bluer. V2 is likely an RR Lyrae star of the M31 field.

V4—The V light curve is sparsely sampled between phase 0.40 and 0.70. However, maximum and minimum light are well covered, hence the intensity-averaged mean V magnitude should be correct. The star is about 1.5 mag brighter than the HB, and in the PW plane V4 falls within 1σ from the relation for FO ACs, but also fits well the relation for fundamental-mode CCs.

V6—Due to the star pulsation period ($P = 1.067$ days) and our data sampling, we do not have data points in the rising part of the light curve both in B and V. This affects the star

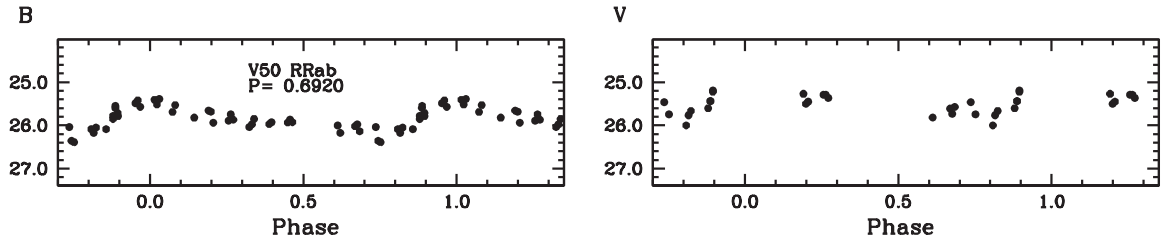

Figure 1. (Continued.)

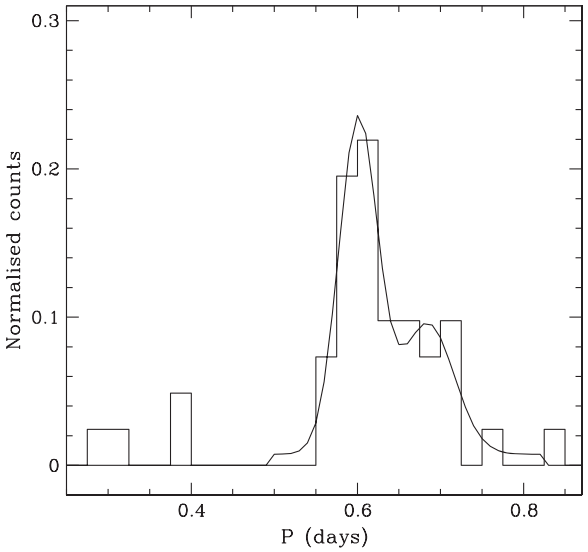

Figure 2. Histogram of the periods of the RR Lyrae stars identified in And XXI. The bin size is 0.025 days. The Gaussian fit to the period histogram is also shown. The two stars at $P = 0.8342$ days and $P = 0.756$ days are V8 and V48, respectively.

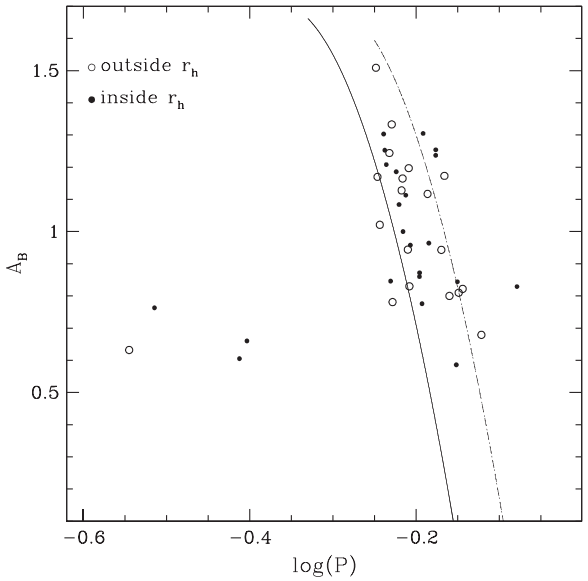

Figure 3. Period-amplitude diagram for the RR Lyrae stars in And XXI. Solid and dashed lines represent the loci defined by bona fide regular and well-evolved RR Lyrae stars in M3 (Cacciari et al. 2005), respectively. Filled and open symbols mark variables within and outside the galaxy half-light radius, respectively.

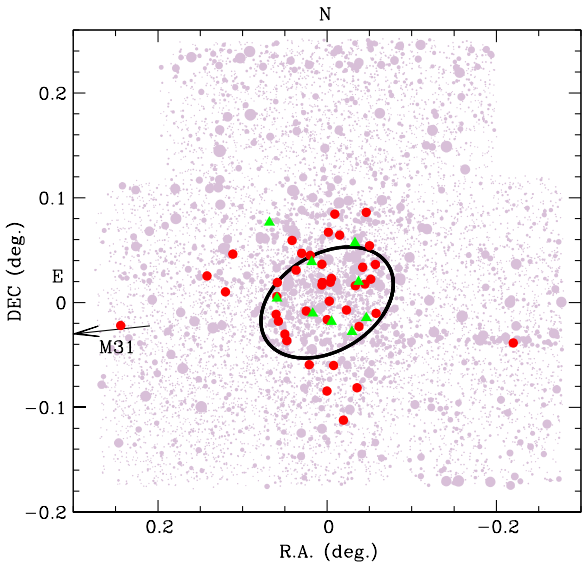

Figure 4. Spatial distribution of the variable stars detected in And XXI. Red filled circles mark the RR Lyrae stars and green filled triangles are the ACs. Symbol size for all other stars is proportional to the magnitude. An ellipse marks the area enclosed in the half-light radius defined by Martin et al. (2009). The arrow marks the direction toward the M31 center.

mean magnitudes. In fact in the PW plane V6 is slightly off the relation for FO ACs.

V8—This is the longest period ($P = 0.8342$ days) and the brightest ($V = 24.93$ mag) RR Lyrae in our sample. It has very similar amplitudes in B and V. V8 is also the reddest variable in And XXI. In Figure 5 V8 is plotted with a star sign, and follows well the PW relation for F-mode ACs, suggesting that this star could be an AC.

V26—As for V6 this AC lacks part of the B and V light curves due to the combination of pulsation period ($P = 1.1500$ days) and sparse data sampling.

V27—This is one of the two brightest RR Lyrae stars in our sample. The B and V amplitudes are small for an RRab of that period ($P = 0.7052$ days); nevertheless, the amplitude ratio $A_B/A_V = 1.28$ is typical of an RR Lyrae star.

V46—The star period is uncertain and the light curves are noisy. However amplitudes and average magnitudes are typical of a normal RR Lyrae star.

V49/V50—These two variables are about 12′ away from the galaxy center. However, the pulsation period and the mean magnitudes are consistent with the average values of the RR Lyrae stars in And XXI. We will show in Section 6 that portions of And XXI seem to extend that far from the galaxy center.

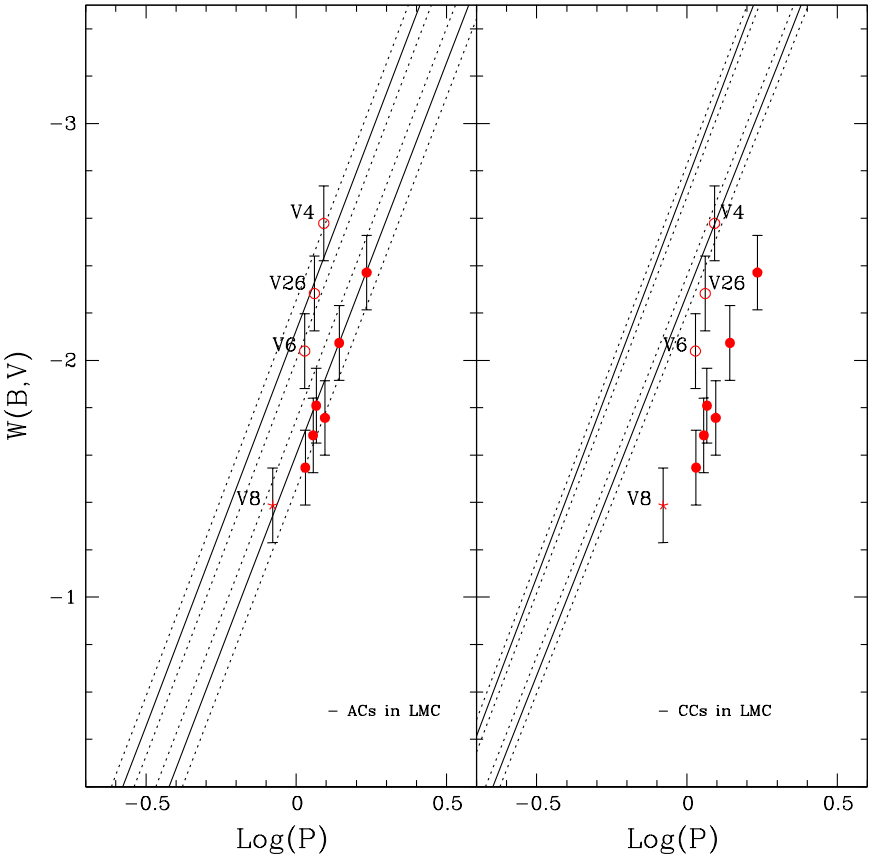

Figure 5. PW relations for the nine variable stars in And XXI that are brighter than the horizontal branch. Red filled circles are fundamental mode pulsators; open red circles are first-overtone variables. Also plotted as a star is the bright RR Lyrae variable V8 (see details in the text). Solid lines in the left panel are the PW relations for ACs in the LMC (Ripepi et al. 2014), while in the right panel are shown the PW relations for CCs in the LMC from Soszynski et al. (2008). Dashed lines show the 1σ contours.

4. DISTANCE

The distribution of the intensity-averaged mean V magnitudes of the RR Lyrae stars in And XXI is shown in the histogram of Figure 7. The average magnitude of the 41 RR Lyrae stars in And XXI is $\langle V(RR)\rangle = 25.33 \pm 0.11$ mag (average on 41 stars). Considering only RR Lyrae stars inside the area defined by the galaxy r_h, the average becomes $\langle V(RR)\rangle = 25.32 \pm 0.13$ mag (average on 22 stars). Among the RR Lyrae stars, V8 and V27 are 0.3 mag brighter than the RR Lyrae average V magnitude and most are probably blended objects or foreground RR Lyrae stars of the M31 halo. On the faint side variables V2 and V9, are ∼0.3 mag fainter than the RR Lyrae average V magnitude and possibly are RR Lyrae belonging either to the M31 halo or to a structure around M31. Excluding these four stars (V2, V8, V9 and V27) the averages we obtain are $\langle V(\mathrm{RR})\rangle = 25.33 \pm 0.06$ mag (average on 37 stars) for all and $\langle V(\mathrm{RR})\rangle = 25.32 \pm 0.12$ mag (average on 19 stars) for the RR Lyrae stars inside the galaxy r_h. We adopt the latter value for the average V magnitude of And XXI RR Lyrae stars, $M_V = 0.54 \pm 0.09$ mag for the absolute visual magnitude of RR Lyrae stars with a metallicity of [Fe/H] = −1.5 dex (Clementini et al. 2003) and $\Delta M_V/\Delta[\mathrm{Fe/H}] = 0.214 \pm 0.047$ mag dex^{-1} (Clementini et al. 2003; Gratton et al. 2004) for the slope of the RR Lyrae luminosity–metallicity relation. For And XXI metallicity we adopt the value [Fe/H] = −1.8 ± 0.4 dex as derived spectroscopically by Collins et al. (2013). To correct for interstellar extinction we derived the reddening from the galaxy RR Lyrae stars using the method by Piersimoni et al. (2002). This is based on the relation between intrinsic $B - V$ color, period, amplitude of the luminosity variation in the B band, and metallicity of the RR Lyrae stars. The reddening value we derive is $E(B - V) = 0.15 \pm 0.04$ mag, assuming [Fe/H] = −1.8 dex for the metallicity. The $E(B - V)$ value and its rms do not change if stars V2, V8, V9, and V27 are excluded. The $E(B - V)$ derived from the RR Lyrae stars is larger than the value of $E(B - V) = 0.094 \pm 0.026$ mag derived by Schlegel et al. (1998), but still consistent in 1σ. The distance modulus of And XXI derived from the RR Lyrae stars using our reddening estimate is $(m - M)_0 = 24.40 \pm 0.17$ mag. Our distance modulus is smaller than the one found by Conn et al. (2012)[$(m - M)_0 = 24.59^{+0.06}_{-0.07}$ mag] using the luminosity of the RGB tip, although compatible within 1σ. The difference between the two distance estimates is mostly due to differences in the adopted reddening values. Conn et al. (2012) use the reddening by Schlegel et al. (1998), which is 0.057 mag smaller than our estimate from the RR Lyrae stars. If one adopts the same reddening value, the two distance moduli become identical.

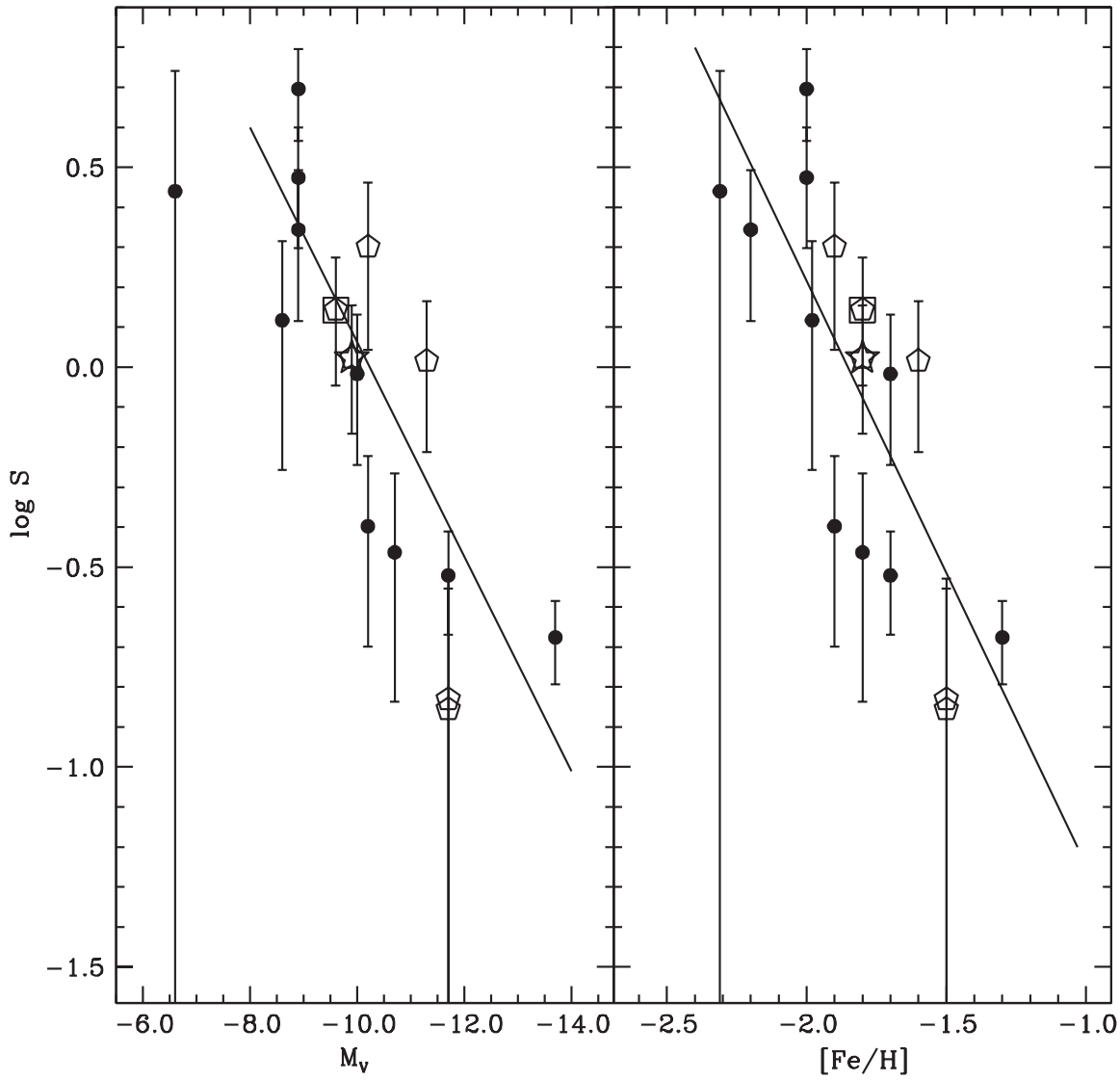

Figure 6. Left: specific frequency of ACs in dwarf satellites of the MW (filled circles) and M31 (open pentagons) vs. absolute visual magnitude. And XXI is represented by a starred symbol, And XIX by an open square. The black lines in both panels are the best fits to the data. Right: same as in the left panel, but vs. metallicity of the parent galaxy.

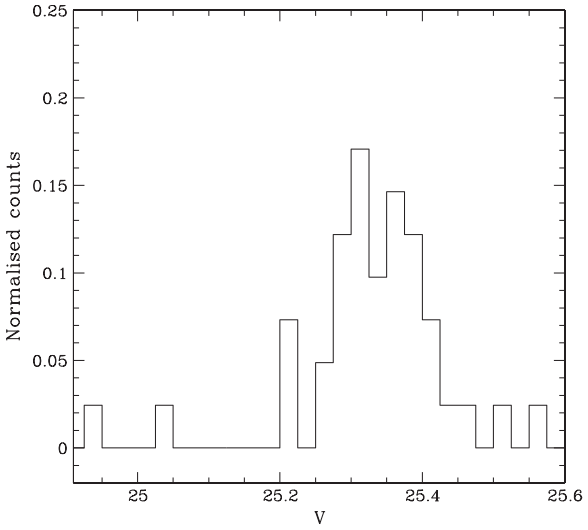

Figure 7. Histogram of the intensity-averaged mean V magnitudes of the RR Lyrae stars identified in And XXI. The bin size is 0.025 mag. The two brightest stars are V8 and V27, the two faintest ones are V2 and V9.

5. CMD AND STELLAR POPULATIONS

The CMD of And XXI obtained in the present study is shown in Figure 8, where in the left panel we plotted only sources located within the area delimited by the galaxy half-light radius and the ellipticity by Martin et al. (2009), whereas the right panel shows the CMD of all sources in the LBC field of view (FOV). To mitigate contamination from background galaxies and peculiar objects we selected our photometric catalog using the χ and Sharpness quality parameters provided by ALLFRAME and only retained sources with $-0.3 \leqslant$ Sharpness $\leqslant 0.3$ and $\chi < 1.1$. The variable stars are plotted with red filled circles and green triangles for RR Lyrae stars and ACs, respectively. Prominent features of the CMD are the blue HB traced by the RR Lyrae stars, the red HB, and the RGB. The sequence of stars at $B - V \sim 1.5$–1.7 mag and extending blueward around $V = 22$ mag is mostly composed by foreground field stars. The relative occurrence of both RR Lyrae stars and ACs in And XXI suggests that the galaxy hosts different stellar generations. The CMD features and the position of the

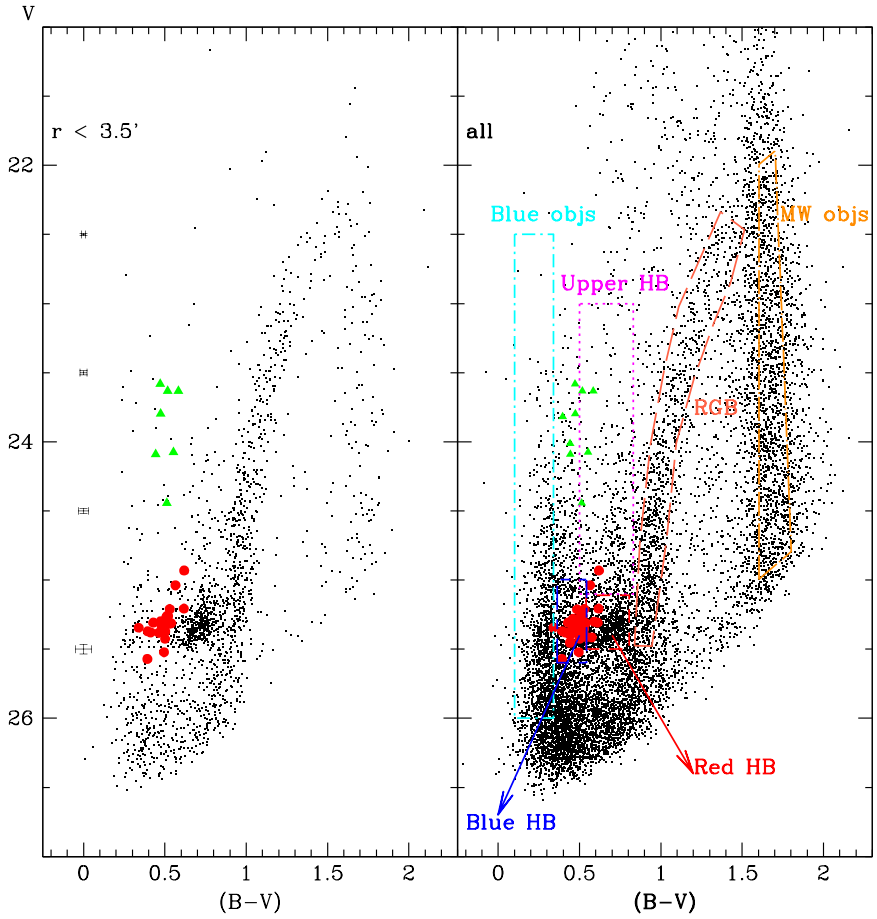

Figure 8. Left: CMD of the sources in our photometric catalog with $-0.3 \leqslant$ Sharpness $\leqslant 0.3$, $\chi < 1.1$ and located within the area delimited by the galaxy half-light radius and the ellipticity by Martin et al. (2009). Red circles mark the RR Lyrae stars while the green triangles are ACs. Typical error bars are shown on the left. Right: as in the left panel, but considering sources in the whole LBC FOV. The regions in the CMD mark different selections performed to study the *projected* distributions (see Section 6).

variable stars in the CMD were compared to the Padova isochrones obtained using the CMD 2.5 web interface (http://stev.oapd.inaf.it/cgi-bin/cmd) that is based on models from Bressan et al. (2012). This is shown in Figure 9. Isochrones from 11 to 13 Gyr and $Z = 0.0003$ fit well the blue part of the RGB and the position of the RR Lyrae stars, (see top panels of Figure 9). Bressan et al. (2012) use for the Sun a value of $Z = 0.0152$; hence, the tracks at $Z = 0.0003$ correspond to [Fe/H] $= -1.7$ dex. The central and red part of the RGB together with red HB are well fitted by isochrones from 6 to 10 Gyr and enhanced metallicity ranging from $Z = 0.0004$ to $Z = 0.0006$ ([Fe/H] ~ -1.5 dex), as shown in the central and bottom panels of Figure 9. The intermediate age population seems to be dominant in And XXI given the best fit of the RGB with the 6–10 Gyr isochrones and the high number of HB-red stars (692) compared to HB-blue stars (368), and also considering that the contamination by background unresolved galaxies is much more prominent in the HB-blue. Another possible argument in favor of this hypothesis is the paucity of RRc stars. In the literature there are other systems with similar properties of metallicity and average period of the RRab stars that totally lack RRc stars, the Galactic globular clusters Ruprecht 106 (Rup 106; Kaluzny et al. 1995) and NGC 5824 (Meissner & Weiss 2006) that are both younger than other Galactic globular clusters with the same metallicity.

The presence in And XXI of nine ACs gives hints of a possible stellar population with an age in the range of 1–2 Gyr. Indeed, Figure 10 shows that the position of the ACs in the CMD is well fitted by isochrones from 1 to 2 Gyr with metallicity in the range $Z = 0.0001$–0.0006. Furthermore, above the HB we observe a sequence of objects that likely belongs to this young stellar component. We should remind that the origin of ACs is still a matter of debate in the literature, with the two most accepted scenarios being that they either represent young single stars produced by a relatively recent episode of star formation, or that they formed from mass transfer in binary systems as old as the other stars in the galaxy. Both channels may produce ACs; however, perhaps a distinction can be made between the few ACs found in old stellar systems like globular clusters and ultra-faint dwarf galaxies (UFDs) like Hercules (Musella et al. 2012), which likely originate from binaries, and the larger numbers of ACs found in galaxies with gas and recent star formation like Leo T (Clementini et al. 2012) among the UFDs and And XIX (Paper I) and And XXI among the M31 satellites, which likely are bona fide young stars.

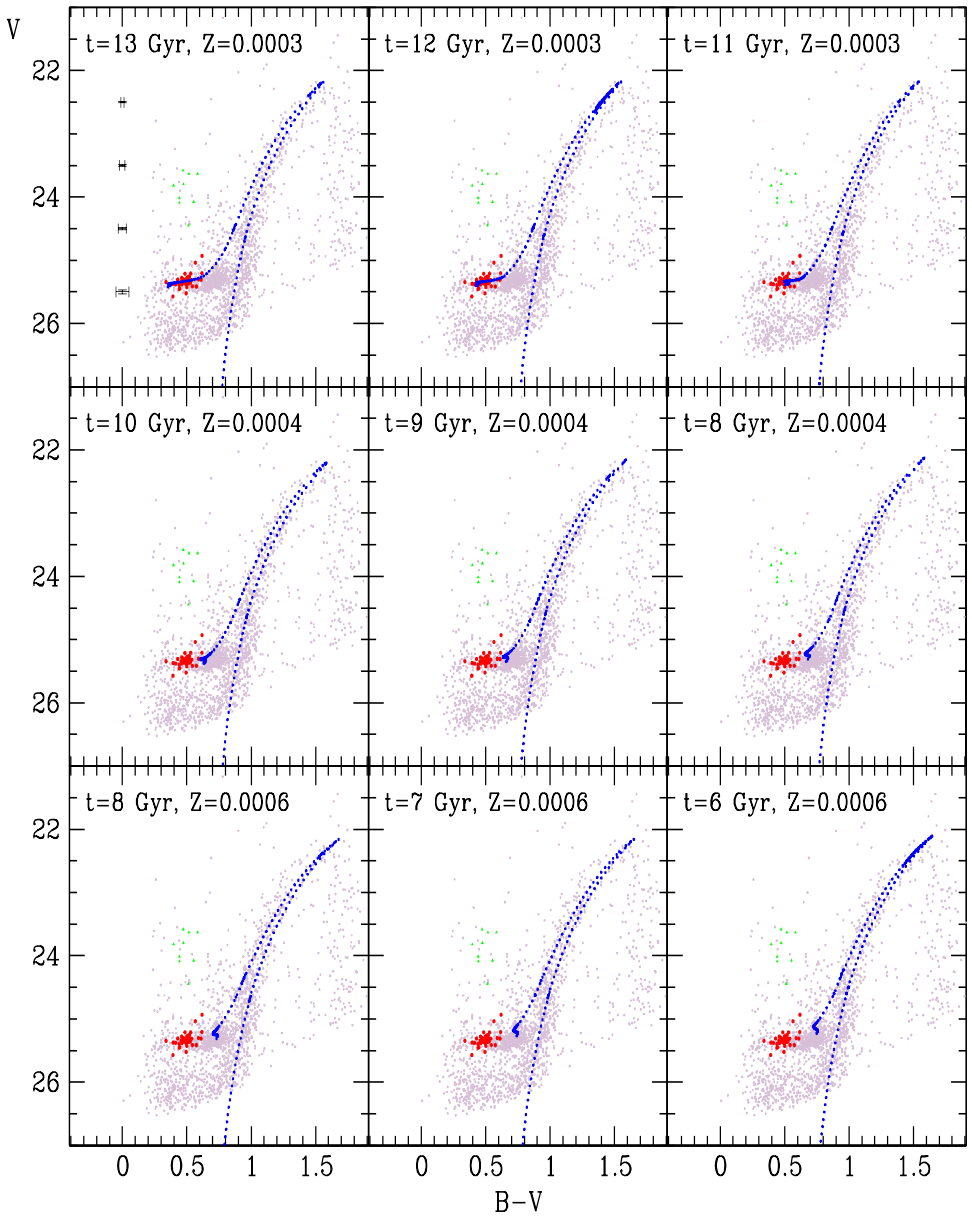

Figure 9. CMD of And XXI overlaid by Padova stellar isochrones (Bressan et al. 2012) with different age (13–6 Gyr) and metallicity ($Z = 0.0003$, $Z = 0.0004$ and $Z = 0.0006$; from top to bottom). Red filled circles are RR Lyrae stars, the green filled triangles are ACs.

6. PROJECTED DISTRIBUTIONS

To check whether the objects above the HB are young stars belonging to And XXI and not contaminant sources, we selected stars from the CMD of all the sources in the LBC FOV that have color in the range $0.50 < (B - V) < 0.83$ mag and magnitude $23.0 < V < 25.1$ mag (see the right panel of Figure 8 for the different selections). We plotted the selected objects in an R.A. and decl. map (see the bottom left panel of Figure 11) and found evidence of a clustering about ∼1 arcmin ($0.^{\circ}017$) south–west from And XXI center. Although slightly offset with respect to the center of And XXI these young objects correlate with the general *projected* distribution of the CMD-selected RGB and red-HB stars, as shown in Figure 11, and likely are galaxy members. The distribution of RGB stars (middle left panel of Figure 11) is consistent with And XXI position angle and ellipticity as given by Martin et al. (2009), while the red-HB stars (middle right panel of Figure 11) appear to be more concentrated toward the center than the RGB stars. That older stars have a more extended distribution compared to younger populations is a well known, general feature seen in dwarf galaxies (see, e.g., Held et al. 2001; Tolstoy et al. 2004; Clementini et al. 2005; Bellazzini et al. 2014).

The blue objects between $0.1 < (B - V) < 0.4$ mag and $22.5 < V < 26$ mag are most probably unresolved galaxies, as discussed in Paper I. Their *projected* distribution (top right panel in Figure 11) is homogeneous over the whole LBC FOV, hence confirming that they are contaminant sources. The red objects between $1.5 < (B - V) < 2.1$ mag and $26 < V < 21$ mag are MW foreground stars and are equally distributed all over the FOV (top left panel in Figure 11). Since there is a strong contamination from unresolved

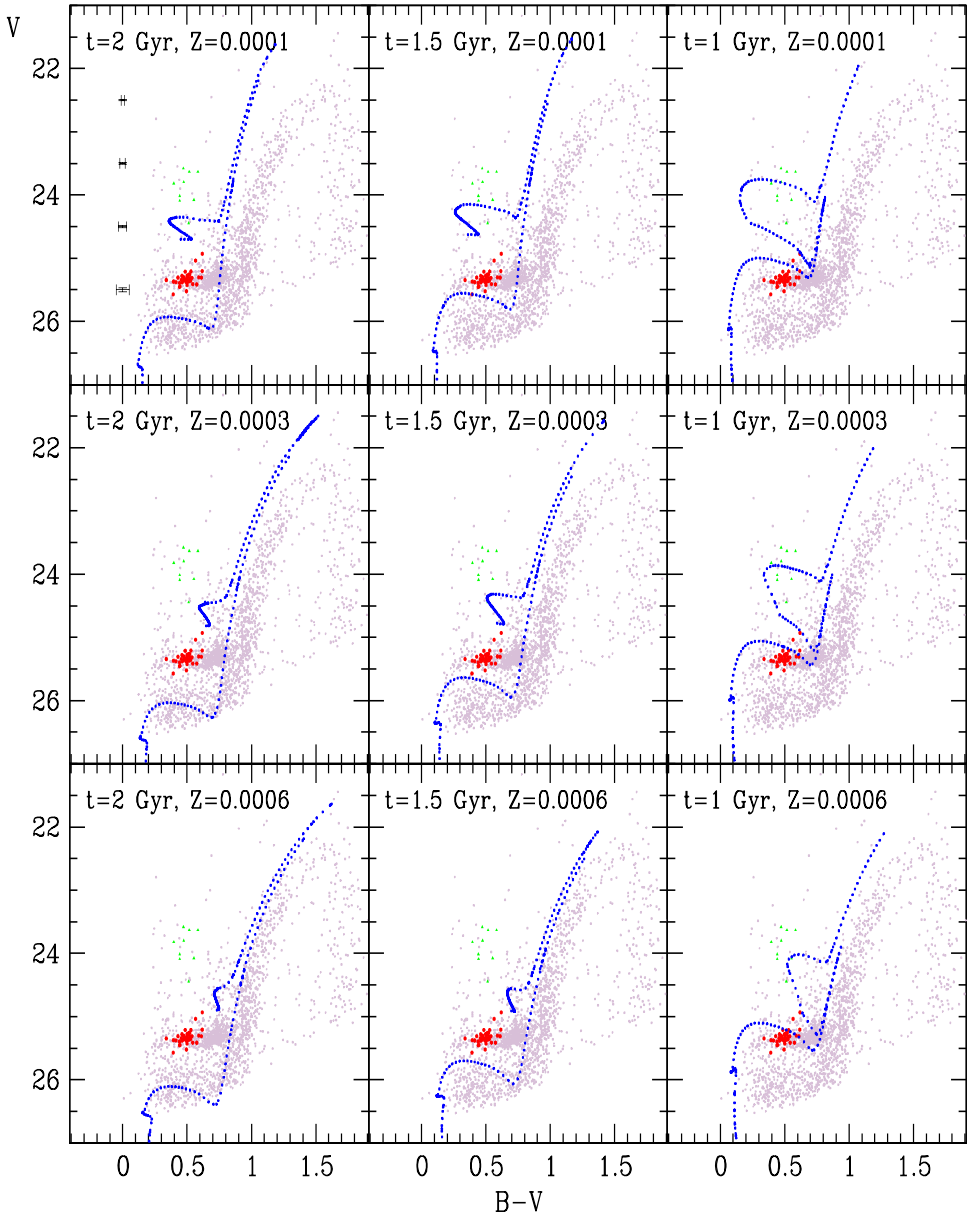

Figure 10. Same as in Figure 9, but for isochrones of 1, 1.5, and 2 Gyr and metallicity $Z = 0.0001$, $Z = 0.0003$, and $Z = 0.0006$ (from top to bottom).

galaxies in the blue part of the CMD, it is a hard task to separate out the blue-HB members of And XXI. We selected as blue-HB members the stars falling in the CMD region $0.35 < (B - V) < 0.65$ mag and $25.2 < V < 25.7$ mag, as defined by the RR Lyrae variables identified in this work. In the *projected* distribution, the blue HB stars (bottom right panel in Figure 11) are spread almost homogeneously over the galaxy and although the contamination from background sources may be significant, the HB-selected stars follow the galaxy position angle.

In order to identify particular structures in And XXI, we built isodensity maps of the RGB, red-HB, and upper-HB stars. They are shown in Figure 12. Stars were binned in $1\farcm2 \times 1\farcm2$ boxes and smoothed by a Gaussian kernel of FWHM of $1\farcm2$ ($0\fdg02$). The first contour levels are 3σ above the sky background. Directions to M31 and And XIX, which is the biggest satellite in the neighborhood of And XXI, are also shown in the figure. The *projected* relative distance of And XXI to M31 and And XIX is of ∼130 and ∼100 kpc, respectively. The RGB stars are spread over the LBC FOV for more than twice the galaxy r_h. This was already clear for the presence of RR Lyrae stars far from the galaxy center. Up to 6–7 arcmin ($\sim 0\fdg11$) from the center the isodensity contours well follow the position angle given by Martin et al. (2009). Right after 7 arcmin the isodensities appear to be twisted and in the east part of the LBC FOV are distorted in the direction of And XIX. A sort of arm highlighted by the presence of one RR Lyrae star extends in the direction of M31. The contours of red-HB and RGB stars have a similar distribution, while the upper-HB stars have different center and orientation when compared to the other two populations. The three populations show overdensities in the

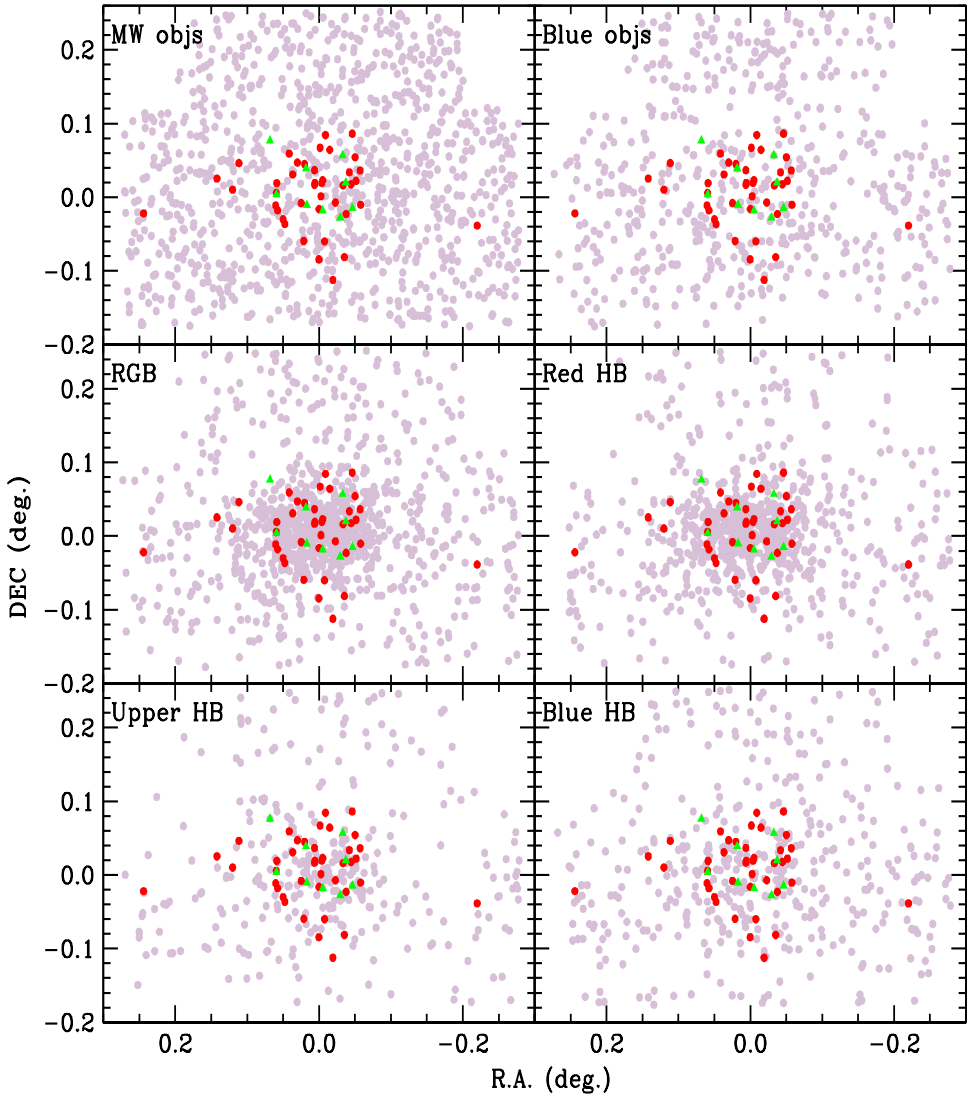

Figure 11. Projected distribution of selected samples of objects in the CMD of the total LBC FOV. Superimposed are the RR Lyrae stars (red, filled circles) and the ACs (green, filled triangles).

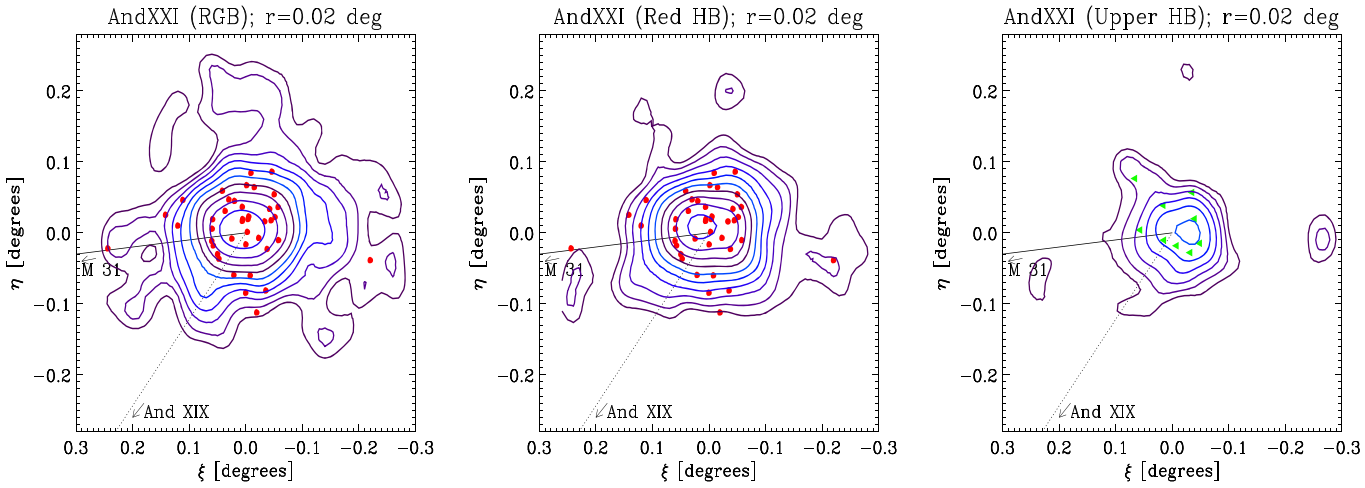

Figure 12. Isodensity contours of three selected samples of stars in And XXI. ξ and η are the R.A. and decl. computed from the center of the galaxy given by Martin et al. (2009) and r is the FWHM of the Gaussian kernel. Left panel: RGB stars, Center panel: red-HB stars, Right panel: upper-HB stars. RR Lyrae stars and ACs are also plotted as red filled circles and green filled triangles, respectively.

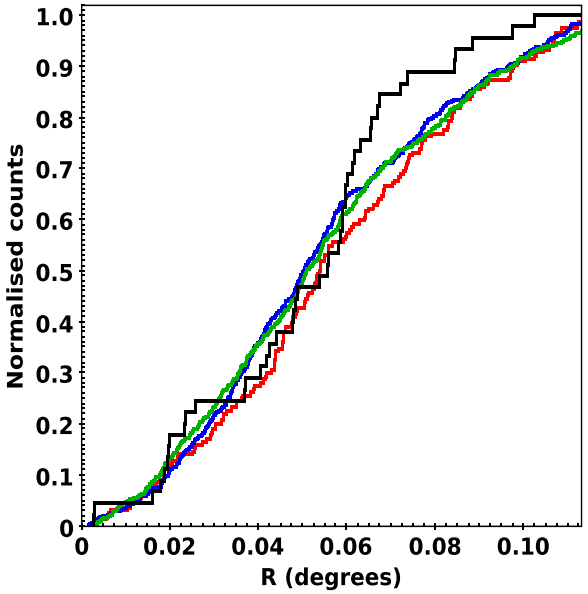

Figure 13. Cumulative radial distributions of selected samples of sources in the CMD of And XXI. Green line: cumulative distribution for the RGB stars; blue line: distribution of the red-HB stars; red line: distribution of the upper-HB sources; black line: distribution of the variable stars.

east, north, and west directions. Two RR Lyrae stars are located at the position of the east and west overdensities, thus endorsing the presence of sub-structures far from And XXI's center.

Figure 13 shows the cumulative radial distributions of selected samples of stars located inside twice the r_h of And XXI. We performed a two-sample Kolmogorov–Smirnov (K–S) test between these radial distributions. The RGB (green line) and red-HB star (blue line) distributions shown in Figure 13 are indistinguishable and likely arise from the same stellar generation. In fact, the K–S test provides a p-value as large as $p = 0.84$, whereas the K–S test between upper-HB population (red line) and RGB stars gives a p-value of only $p = 0.24$.

Finally, though the number of variables (RRLs+ACCs) is very small when compared to the number RGB stars the K–S test gives $p = 0.49$ between the two samples.

7. MERGING?

In Section 3.1 we showed the presence of two peaks in the period distribution of And XXI RRab stars. The double peak in the period distribution can be a clue for the presence of two separate populations of RR Lyrae stars, with slightly different age and/or metallicity. Selecting stars with period within 1σ from the two peaks in period, we find an average magnitude

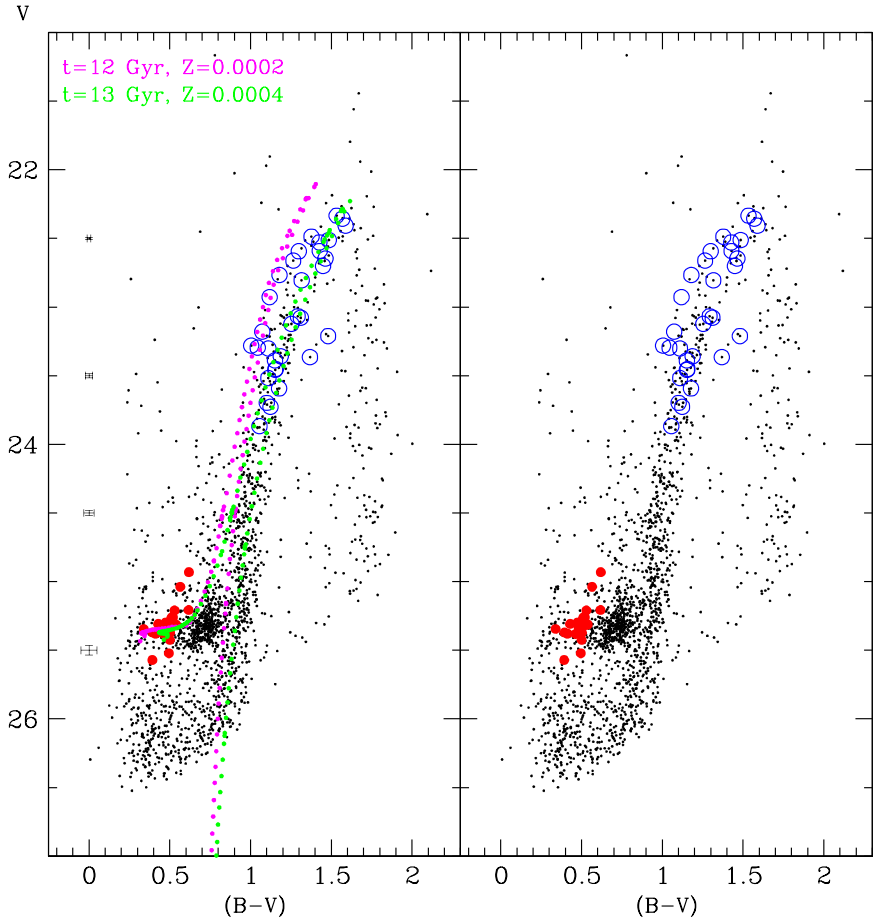

Figure 14. CMD of And XXI marked as open blue circles stars with membership spectroscopically confirmed by Collins et al. (2013). Dashed lines are the Bressan et al. isochrones for 12 Gyr, $Z = 0.0002$ (magenta line) and 13 Gyr, $Z = 0.0004$ (green line), respectively. Red filled circles are RR Lyrae stars. Typical photometric error bars are shown on the left.

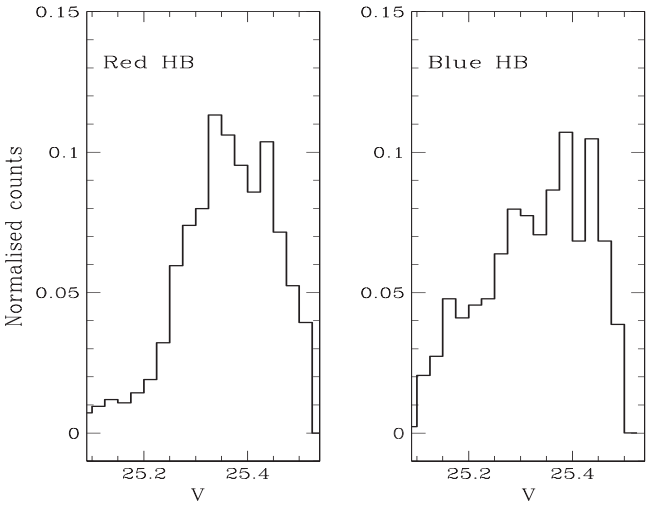

Figure 15. Histogram of the V magnitudes for the stars in the red (left panel) and blue (right panel) HB.

of $V = 25.35 \pm 0.08$ mag for stars with $P_1 = 0.60$ ($\sigma = 0.02$) days and $V = 25.25 \pm 0.10$ mag for stars with $P_2 = 0.68$ ($\sigma = 0.03$) days. Although the 0.1 mag difference between P_1 and P_2 RR Lyrae stars is within the range of errors, it goes in the direction that the longer period RR Lyrae stars (P_2) are brighter than the shorted period (P_1) ones, possibly due to a lower metal content. A difference in metallicity of 0.4 dex can explain such a magnitude difference according to Clementini et al. (2003) and Gratton et al. (2004) slope of the luminosity–metallicity relation of RR Lyrae stars. Since the RR Lyrae stars are produced by a population older than 10 Gyr, the double-peaked period distribution might suggest that either the primordial environment of And XXI was enriched in only 2 Gyr or that the galaxy RR Lyrae stars arise from two different small galaxies that merged to form And XXI.

Furthermore, the RGB of And XXI seems to be bifurcated, giving a further hint for the presence of two slightly different old populations. To show that the spread of And XXI RGB is real and not due to contamination or photometric errors, we matched our catalog with the list of spectroscopic members of And XXI identified by Collins et al. (2013). The latter are marked by blue open circles in the CMD of Figure 14. They are mostly RGB stars that exhibit a wide spread in color, at a given luminosity, due to age and/or metallicity differences. As shown in the left panel of Figure 14 the member stars are enclosed within the 12 Gyr, $Z = 0.0002$ and the 13 Gyr, $Z = 0.0004$ tracks. In addition the red-HB of And XXI also separates in two clumps with a difference of ~0.15 in V magnitude (see the left panel of Figure 15). A further argument in support of the merging scenario is the different

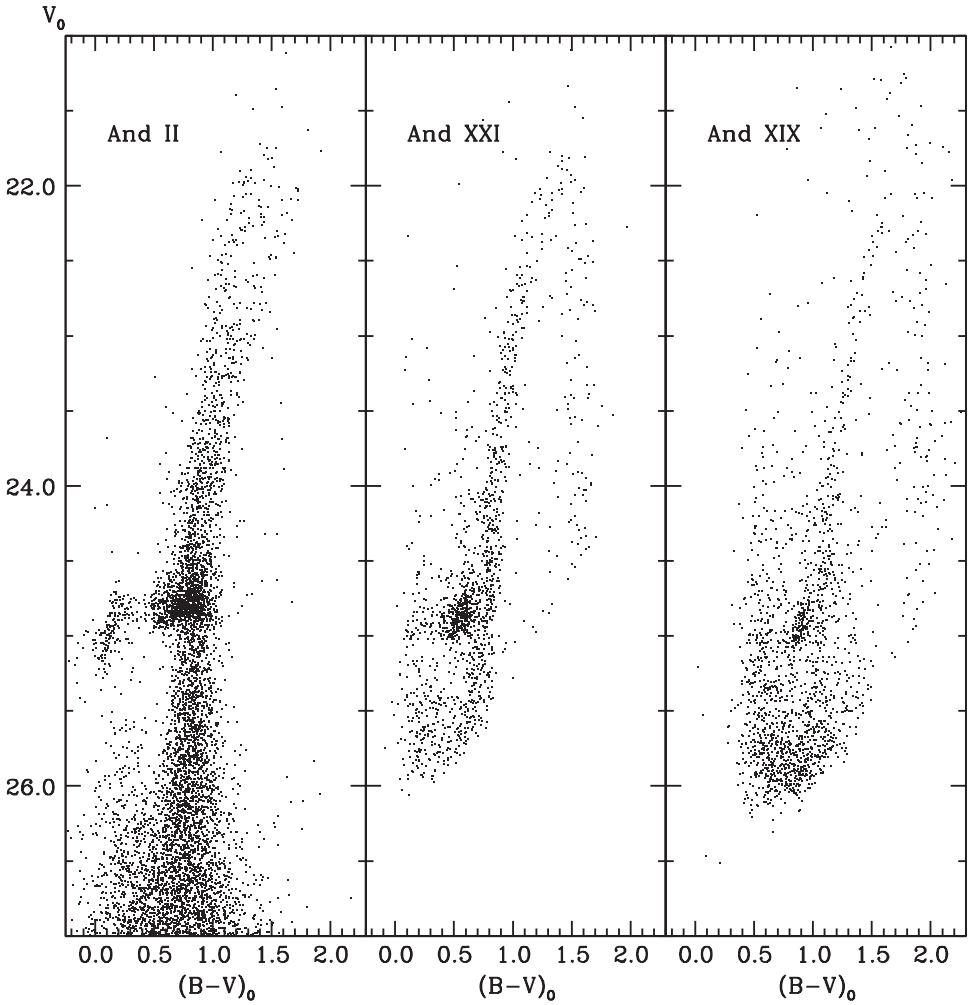

Figure 16. Comparison of the de-reddened CMD of And II (left panel) we obtained from *HST* archive data, with the CMDs of And XXI (central panel; this work) and And XIX (Paper I). Only stars within the respective half-light radii are shown for And XXI and And XIX.

projected distributions of the selected samples of stars in And XXI.

As was earlier suggested by Coleman et al. (2004) and later supported by Yozin & Bekki (2012) with numerical simulations, the MW dSph galaxy Fornax resulted from the merging of two dwarf galaxies. The visible remnant of this collision was detected by Coleman et al. (2004) as a small overdensity of young stars forming a shell structure displaced from Fornax center. The young stars in And XXI (see Section 5) are indeed located in an aggregation displaced from the center of the galaxy, which resembles the overdensity found in Fornax by Coleman et al. (2004). Furthermore, And XXI variable stars seem to be placed in separate shells around the galaxy center (see Figure 4). These features suggest also for And XXI a merging scenario.

According to Amorisco et al. (2014), among the M31 satellites, And II is another example of a dwarf merging remnant. This would explain the stellar stream they detected kinematically in the galaxy. The presence of two different old populations in And II is also supported by the analysis of the CMD and by the properties of the variable stars. The RR Lyrae stars of And II were studied by Pritzl et al. (2004). Using the periods in Table 2 of Pritzl et al. (2004), we performed a multi-Gaussian fit and found two separate peaks, a first one at $P = 0.52$ days with $\sigma = 0.05$ days and a second one at $P = 0.68$ days with $\sigma = 0.01$ days. Hence, similarly to And XXI, And II also seems to host two distinct old stellar populations with different metallicity/age and corresponding different RR Lyrae populations, likely belonged to the two galaxies that merged in the past. The left panel of Figure 16 shows the CMD of And II we obtained using *Hubble Space Telescope* archive data (Prop ID 6514, PI: Gary Da Costa). The galaxy RGB clearly bifurcates in two arms and blue and red HBs also seem to split. CMD and variable stars in And II show properties very similar to And XXI (central panel of Figure 16). For comparison the right panel of Figure 16 shows the de-reddened CMD of And XIX (Paper I) inside the galaxy r_h of 6.2 arcmin. The r_h of And XIX is approximately twice that of And XXI and the contamination by foreground and background objects is much higher. Still the RGB of And XIX is much narrower than the RGB of And XXI and And II. In conclusion, we speculatively attribute some of the features of the CMD and RR Lyrae population of And XXI to the presence of two slightly different stellar populations belonging to two dwarf galaxies that merged in the past.

Recently, Deason et al. (2014) investigated the frequency of merging between dwarf galaxies in the LG using the ELVIS simulations. They found that the frequency of satellite–satellite merging in the host virial radius of the MW and M31 is of the order of 10% and that this frequency doubles for satellites outside the virial radius. Considering the large number of satellites surrounding the MW and M31 these predictions are consistent with both And II and And XXI being the result of satellite merging.

8. CONCLUSIONS

We have discovered a total of 50 variable stars in And XXI, of which 41 are RR Lyrae stars and 9 are ACs. From the average period of the RRab stars $\langle P_{ab} \rangle = 0.64$ days and the Bailey diagram, we classify And XXI as an Oo-II/Int object. Using the variable stars and the CMD we found evidence for the presence in And XXI of two major stellar populations, a first one 12 Gyr old with [Fe/H] = −1.7 dex and a second, more conspicuous one, with an age of 6–10 Gyr and [Fe/H] = −1.5 dex. Furthermore, the discovery of 9 ACs traces also the presence in And XXI of a stellar population as young as 1–2 Gyr. This is similar to what we found in And XIX (Paper I), but in And XXI the 6–10 Gyr stellar component is much more dominant. Other dwarf satellites of M31 contain RR Lyrae stars as well as prominent red clumps in the CMD (e.g., see the CMD of And I and And III in Figure 1 by Pritzl et al. 2005). Mancone & Sarajedini (2008) found that the population of And V is mostly composed of stars 8–10 Gyr old. Our results on the stellar population of And XXI and And XIX together with the above further literature evidence seem to suggest that a global event triggered star formation in the dwarf galaxy satellites of M31 about 6–10 Gyr ago. An engine triggering this common star formation episode could possibly be the flyby encounter of the MW and M31 reported by Zhao et al. (2013)

The *projected* distribution of sources properly selected from the CMD of And XXI shows the existence of an overdensity of young/intermediate age stars in a region slightly off from the galaxy center. We discussed this evidence in light of And XXI possibly being the result of a merging between two dwarf galaxies. This hypothesis is corroborated by the possible presence in the galaxy of two different RR Lyrae populations as well as peculiar features in the CMD (wide RGB, bifurcated red HB) and from the presence of shell-like structures. If future spectroscopic observations will confirm And XXI to be a merged galaxy, it would become the second such satellite in M31, after And II.

We warmly thank P. Montegriffo for the development and maintenance of the GRATIS software, G. Battaglia for providing the software to compute And XXI's density maps, and A. Veropalumbo for software assistance. Financial support for this research was provided by PRIN INAF 2010 (PI: G. Clementini) and by Premiale LBT 2013. The LBT is an international collaboration among institutions in the United States, Italy, and Germany. LBT Corporation partners are The University of Arizona on behalf of the Arizona university system; Istituto Nazionale di Astrofisica, Italy; LBT Beteiligungsgesellschaft, Germany, representing the Max-Planck Society, the Astrophysical Institute Potsdam, and Heidelberg University; The Ohio State University; and The Research Corporation, on behalf of The University of Notre Dame, University of Minnesota, and University of Virginia. We acknowledge the support from the LBT-Italian Coordination Facility for the execution of observations, data distribution, and reduction.

Facility: LBT

REFERENCES

Amorisco, N. C., Evans, N. W., & van de Ven, G. 2014, Natur, 507, 335
Bailey, S. I. 1902, Annals of Harvard College Observatory, 38, 1
Bellazzini, M., Beccari, G., Fraternali, F., et al. 2014, A&A, 566A, 44
Bressan, A., Marigo, P., Girardi, et al. 2012, MNRAS, 427, 127
Cacciari, C., Corwin, T. M., & Carney, B. W. 2005, AJ, 129, 267
Clementini, G., Cignoni, M., Contreras, R., et al. 2012, ApJ, 756, 108
Clementini, G., Contreras Ramos, R., Federici, L., et al. 2011, ApJ, 743, 19
Clementini, G., Di Tomaso, S., Di Fabrizio, L., et al. 2000, AJ, 120, 2054
Clementini, G., Gratton, R., Bragaglia, et al. 2003, AJ, 125, 1309
Clementini, G., Ripepi, V., Bragaglia, A., et al. 2005, MNRAS, 365, 734
Coleman, M., da Costa, G. S., Bland-Hawthorn, J., et al. 2004, AJ, 127, 832
Collins, M. L. M., Chapman, S. C., Rich, R. M., et al. 2013, ApJ, 768, 172
Conn, A. R., Ibata, R. A., Lewis, G. F., et al. 2012, ApJ, 758, 11
Cusano, F., Clementini, G., Garofalo, A., et al. 2013, ApJ, 779, 7
Deason, A., Wetzel, A., & Garrison-Kimmel, S. 2014, ApJ, 794, 115

Gratton, R. G., Bragaglia, A., Clementini, G., et al. 2004, A&A, 421, 937
Hammer, F., Yang, Y., Fouquet, S., et al. 2013, MNRAS, 431, 3543
Held, E. V., Saviane, I., Momany, Y., Rizzi, L., & Bertelli, G. 2001, ApSSS, 277, 331
Ibata, R. A., Lewis, G. F., Conn, A. R., et al. 2013, Natur, 493, 62
Kaluzny, J., Krzeminski, W., & Mazur, B. 1995, AJ, 110, 2206
Madore, B. F. 1982, ApJ, 253, 575
Mancone, C., & Sarajedini, A. 2008, AJ, 136, 1913
Marconi, M., Fiorentino, G., & Caputo, F. 2004, A&A, 417, 1101
Martin, N. F., Ibata, R. A., McConnachie, A. W., et al. 2013, ApJ, 776, 80
Martin, N. F., McConnachie, A. W., Irwin, et al. 2009, ApJ, 705, 758
McGaugh, S., & Milgrom, M. 2013, ApJ, 775, 139
Meissner, F., & Weiss, A. 2006, A&A, 456, 1085
Milgrom, M. 1983, ApJ, 270, 365
Musella, I., Ripepi, V., Marconi, M., et al. 2012, ApJ, 756, 121
Oosterhoff, P. T. 1939, Obs, 62, 104
Pawlowski, M. S., Famaey, B., Jerjen, H., et al. 2014, MNRAS, 442, 2362
Piersimoni, A. M., Bono, G., & Ripepi, V. 2002, AJ, 124, 1528
Pritzl, B. J., Armandroff, T. E., Jacoby, G. H., & Da Costa, G. S. 2005, AJ, 129, 2232
Pritzl, B. J., Jacoby, G. H., & Da Costa, G. S. 2004, AJ, 127, 318
Ripepi, V., Marconi, M., Moretti, M. I., et al. 2014, MNRAS, 437, 2307
Schlegel, D. J., Finkbeiner, D. P., & Davis, M. 1998, ApJ, 500, 525
Soszynski, I., Poleski, R., Udalski, A., et al. 2008, AcA, 58, 163
Stetson, P. B. 1987, PASP, 99, 191
Stetson, P. B. 1994, PASP, 106, 250
Tolstoy, E., Irwin, M. J., Helmi, A., et al. 2004, ApJL, 617, L119
van den Bergh, S. 1975, Stars and Stellar Systems, 9, 509, ed. A. R. Sandage, M. Sandage, & J. Kristian (Chicago, IL: Univ. Chicago Press)
Yozin, C., & Bekki, K. 2012, ApJ, 756L, 18
Zhao, H., Famaey, B., Lüghausen, F., & Kroupa, P. 2013, A&A, 557L, 3
Zolotov, A., Willman, B., Brooks, A. M., et al. 2009, ApJ, 702, 1058